Dynamical evolution of SN ejecta powered by a central engine in multi-D

Akihiro Suzuki (YITP)
collaborator: Keiichi Maeda (Kyoto U.)

Suzuki & Maeda (2017) MNRAS 466 2633 and recent updates

YUKAWA INSTITUTE FOR THEORETICAL PHYSICS

high-energy astrophysics workshop 2017

Superluminous SNe

- Superluminous supernovae(SLSNe): SNe **10-100 times brighter** than normal SNe (Quimby+2007, Barbary+2009 etc, see Gal-Yam+2012 for review)

- They are found by recent "unbiased" transient survey projects (e.g., Palomar transient factory, Pan-STARRS).

- The following classification based on their optical spectra has been proposed (analogy to standard SNe).

  1)**SLSN-I** : no Hydrogen feature
  2)**SLSN-II** : Hydrogen feature
  3)**SLSN-R** : subclass of SLSN-I, their light curves can be explained by the decay of radioactive ^{56}Ni (e.g., 3M$_\odot$ Ni for SN 2007bi)

- Total radiated energy can be ~ 10^{51} [erg]
  (~ explosion energy of normal CCSNe)

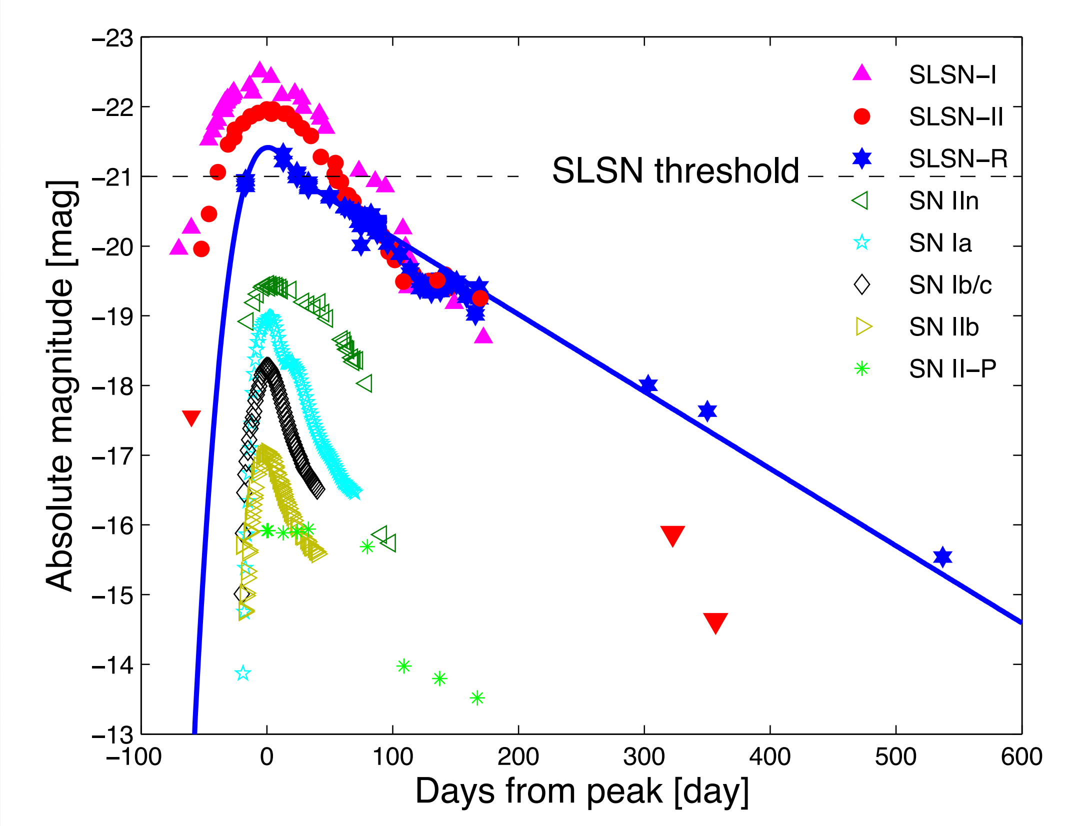

↑light curves of standard SNe, SLSNe (Gal-Yam 2012)

What is the origin of SLSNe-I?

Proposed models and progenitors for SLSNe

- CSM interaction
- pair-instability SNe (very massive progenitor with ~ 100-300$M_\odot$ at ZAMS)
- additional energy injection from the central engine : magnetar spin-down (e.g., Kasen&Bildsten 2010, Woosley 2010) or BH accretion (Dexter&Kasen 2013)


Rotating Neutron Star© ESO

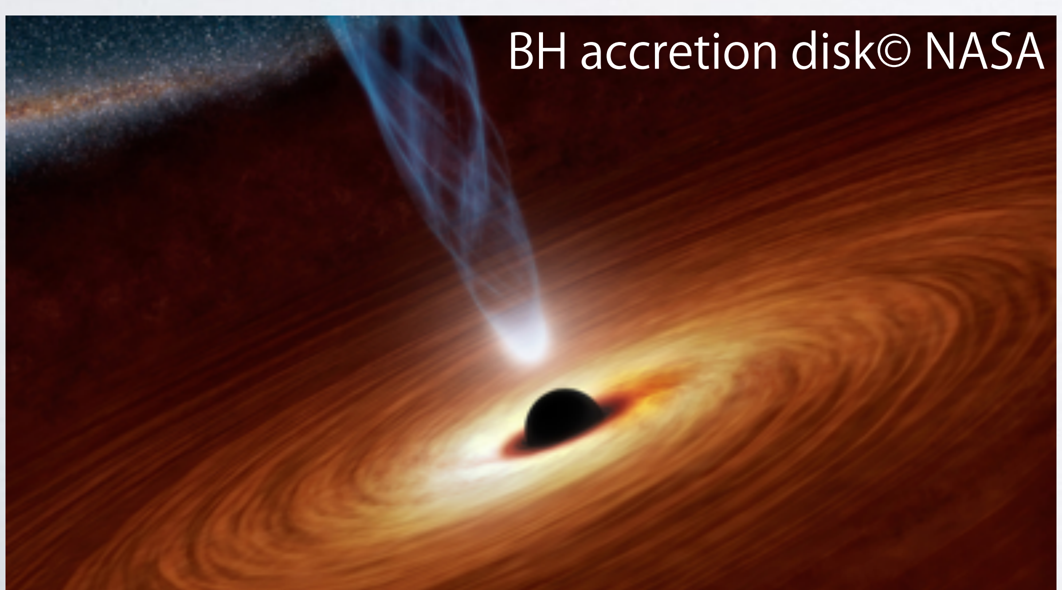
BH accretion disk© NASA

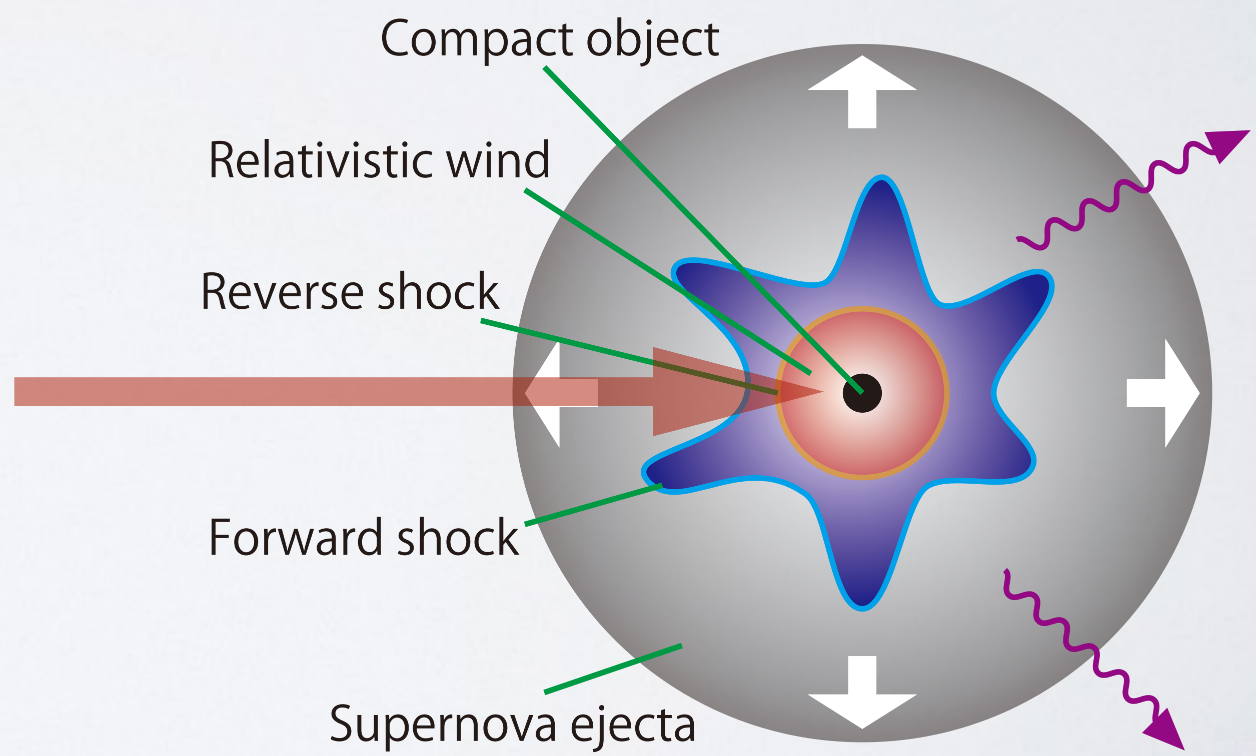

Magnetar scenario

- After the gravitational collapse of the iron core, a massive star experience the core bounce and its outer layer with mass M_{ej} is expelled by neutrino-driven explosion with $E_{kin}=10^{51}$[erg] (standard scenario for CCSNe).

- a neutron star with a strong dipole magnetic field is assumed to form immediately after the neutrino-driven explosion.

radius $R_{\rm ns}$ ~ 10km

moment of inertia $I_{\rm ns} \sim 10^{45}$ g cm^2

initial period of $P_{\rm i} \sim 1$ ms

$E_{\rm rot} = I_{\rm ns}\Omega_{\rm i}^2/2 \simeq 2\times 10^{52}$ erg.

- spin-down of the new-born magnetar is expected to power the SN ejecta

$$L = \frac{E_{\rm rot}/t_{\rm ch}}{(1+t/t_{\rm ch})^2}$$

$$L \simeq \frac{B^2R_{\rm ns}^6\Omega_{\rm i}^4}{6c^3} \sim 10^{49}B_{15}^2R_{\rm ns,6}^6P_{\rm i,-3}^{-4}\ {\rm erg\ s^{-1}}$$

$$t_{\rm ch} = \frac{6I_{\rm ns}c^3}{B^2R_{\rm ns}^6\Omega_{\rm i}^2} = 4.1\times 10^3 I_{\rm ns,45}B_{15}^2R_{\rm ns,6}^6P_{\rm i,-3}^2\ {\rm s}.$$

Magnetar scenario

- one-box light curve model for SNe with magnetar energy injection
- LCs are explained by “tuning” several free parameters, M_{ej}, B, and P_i.
- Magnetar scenario looks successful when one-box model is considered.

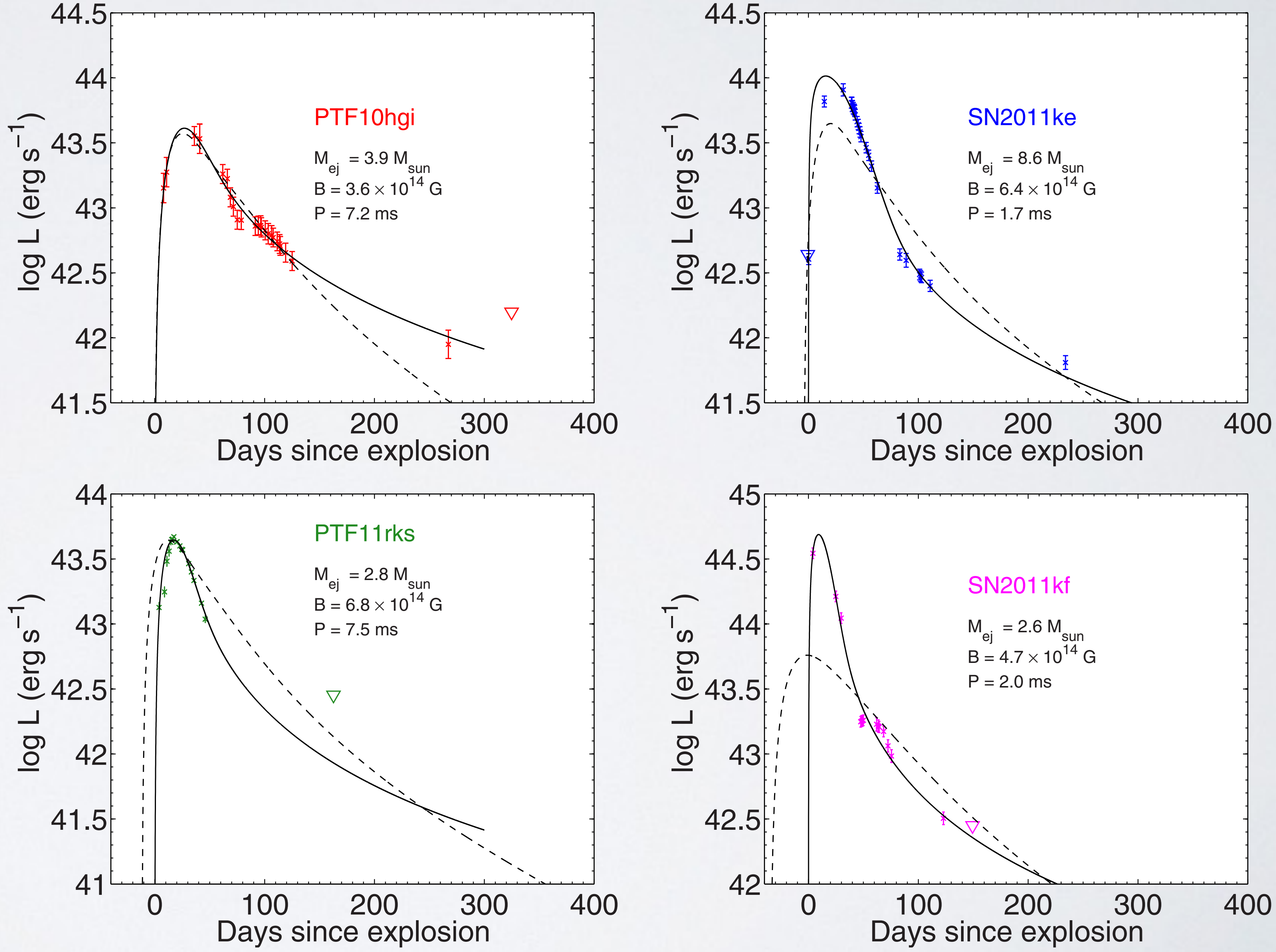

↑Magnetar model fit to SLSNe-I (Inserra+2013)

Magnetar scenario

- one-box light curve model for SNe with magnetar energy injection
- LCs are explained by “tuning” several free parameters, M_{ej}, B, and P_i.
- Magnetar scenario looks successful when one-box model is considered.
- Magnetar fit :

- spin-period ~ 1 - 7 [ms]
- B ~ 10^{13} - a few 10^{14} [G]
- time-scale ~ a few 10-100 days
- E_k ~ 10^{51} - 10^{52} [erg]
- M_{ej} ~ 2 - 10 $M_\odot$

(e.g., Nicholl+2017)

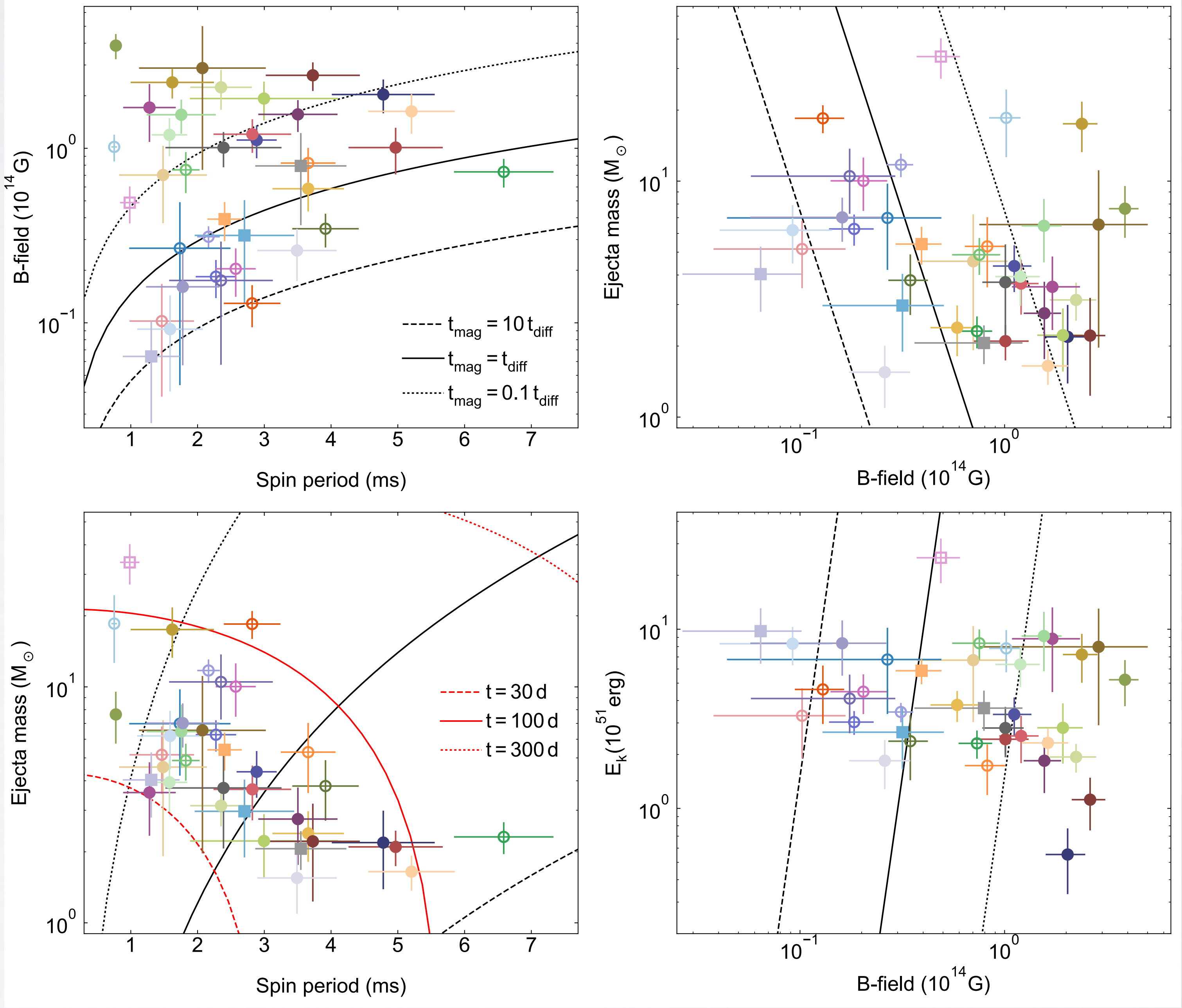

↑Magnetar model fit to SLSNe-I (Nicholl+2017)

Q: But, how the magnetar power the ejecta?

- The magnetic braking is formulated by assuming a **rotating neutron star with a dipole magnetic field** surrounded by **vacuum**. What happens in highly dense environment? Can we apply the vacuum dipole formula?
- OK, we can assume that the energy extraction from the rotating neutron star is realized by the magnetic braking. But, the energy flux is "**Poynting-flux dominated**" → long-standing (notorious) ***σ*** **-problem**: how to convert Poynting-dominated flow to particle energy-dominated flow???
- OK, we can assume the energy flux is dominated by some form (thermal or kinetic) of the particle energy at some distant region. But, **what kind of spectrum** is expected? The flow is composed of electron-positron pair or high energy ions? The flow may also be baryon-rich (no CR or pair acceleration).

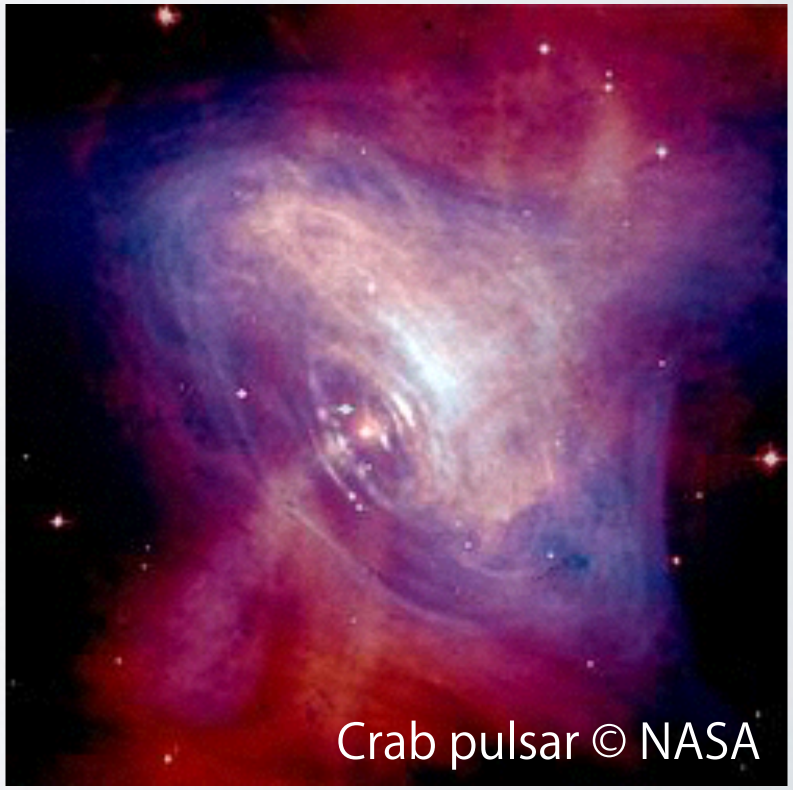

Relativistic wind from magnetized NS

- SN ejecta (or SNR) pushed by a pulsar wind nebula
- e.g., Crab nebula

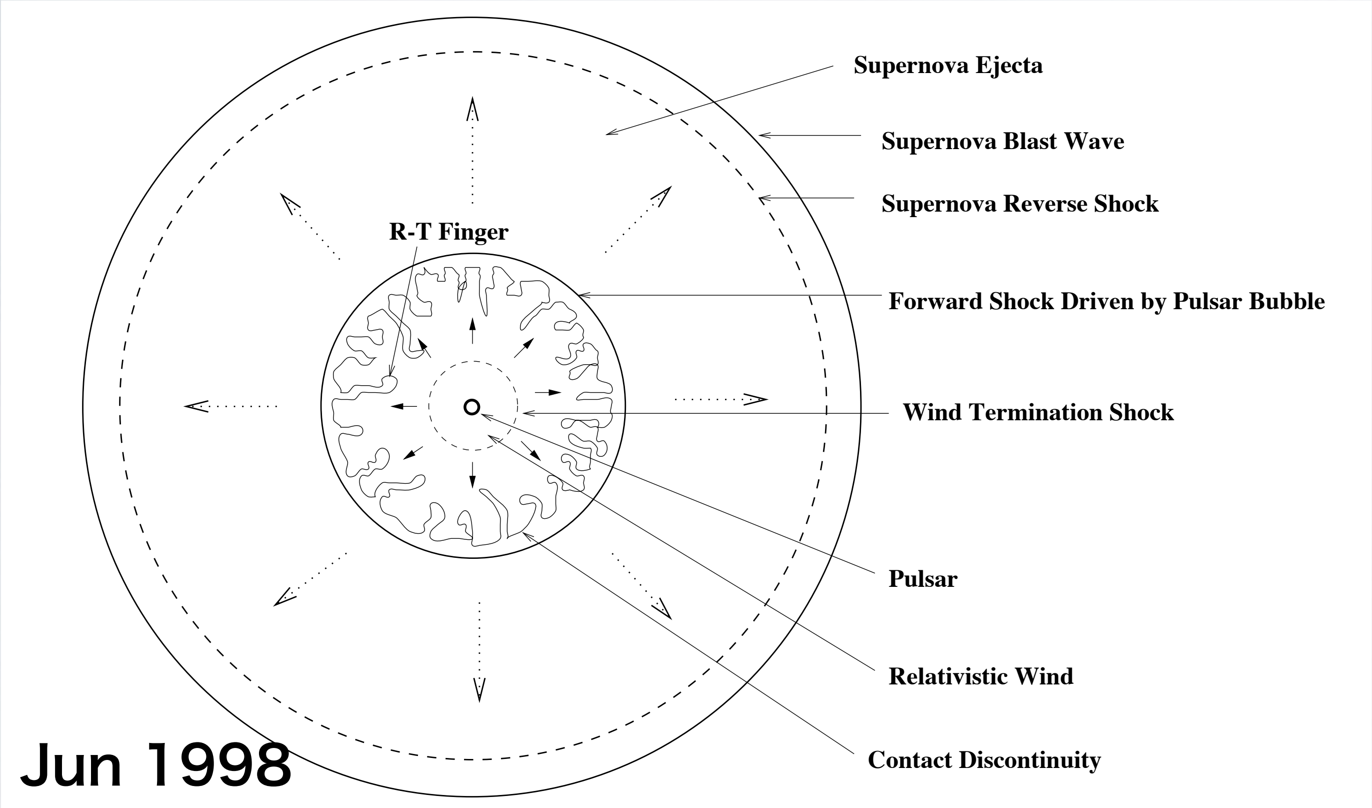

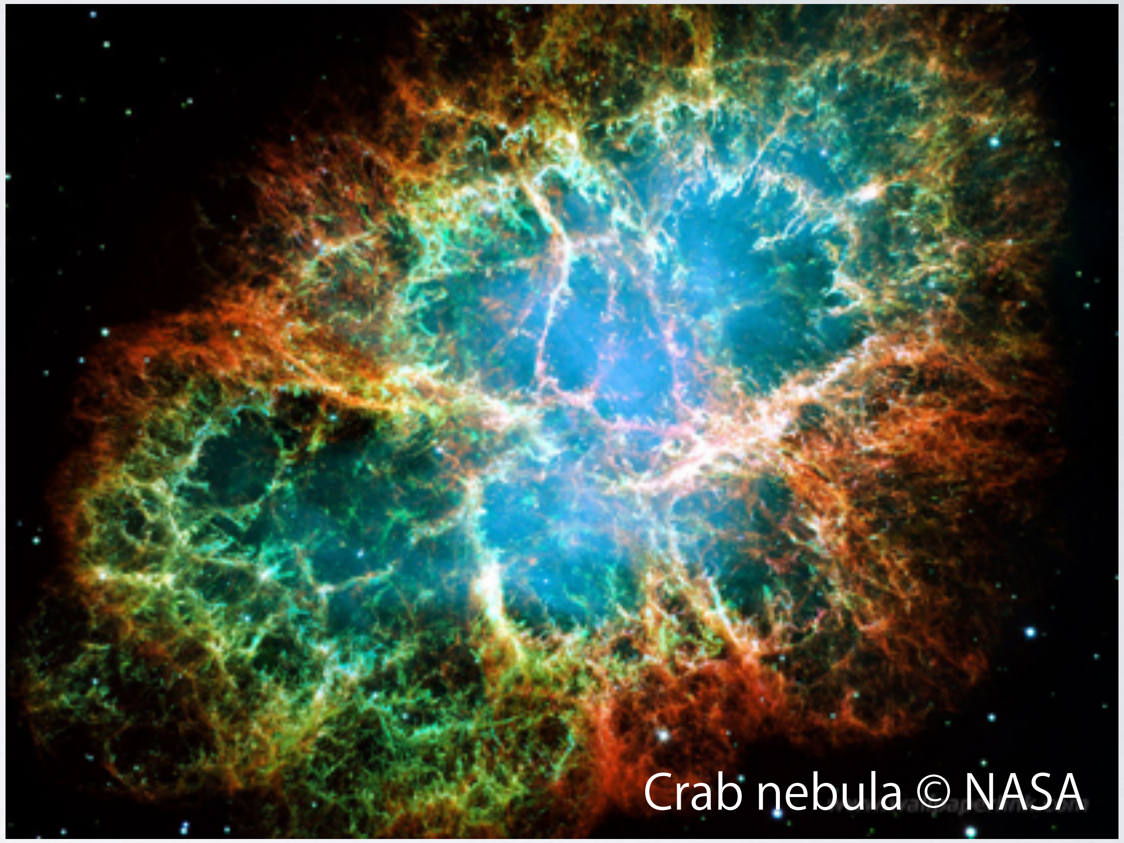

- galactic PWNe: injected energy E_{inj} < SN explosion energy E_{exp}

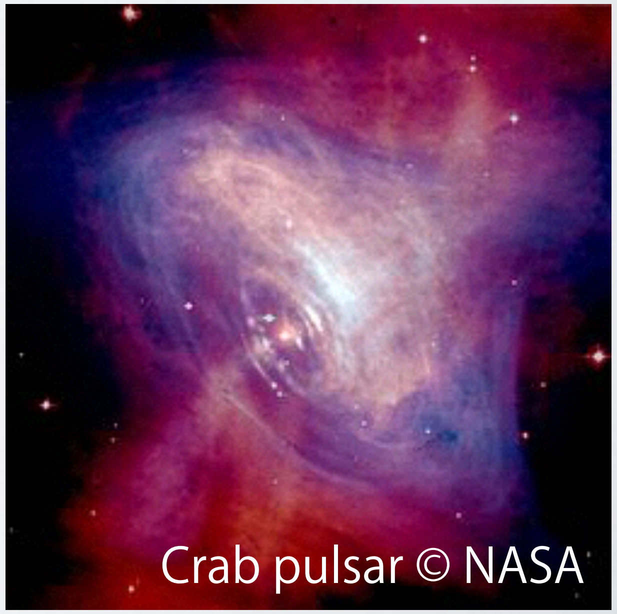

What happens when $E_{inj} > E_{exp}$?
(or maybe $E_{inj} >> E_{exp}$)

1D spherical picture of SN-wind interaction

e.g., Chevalier (1992), Jun (1998)

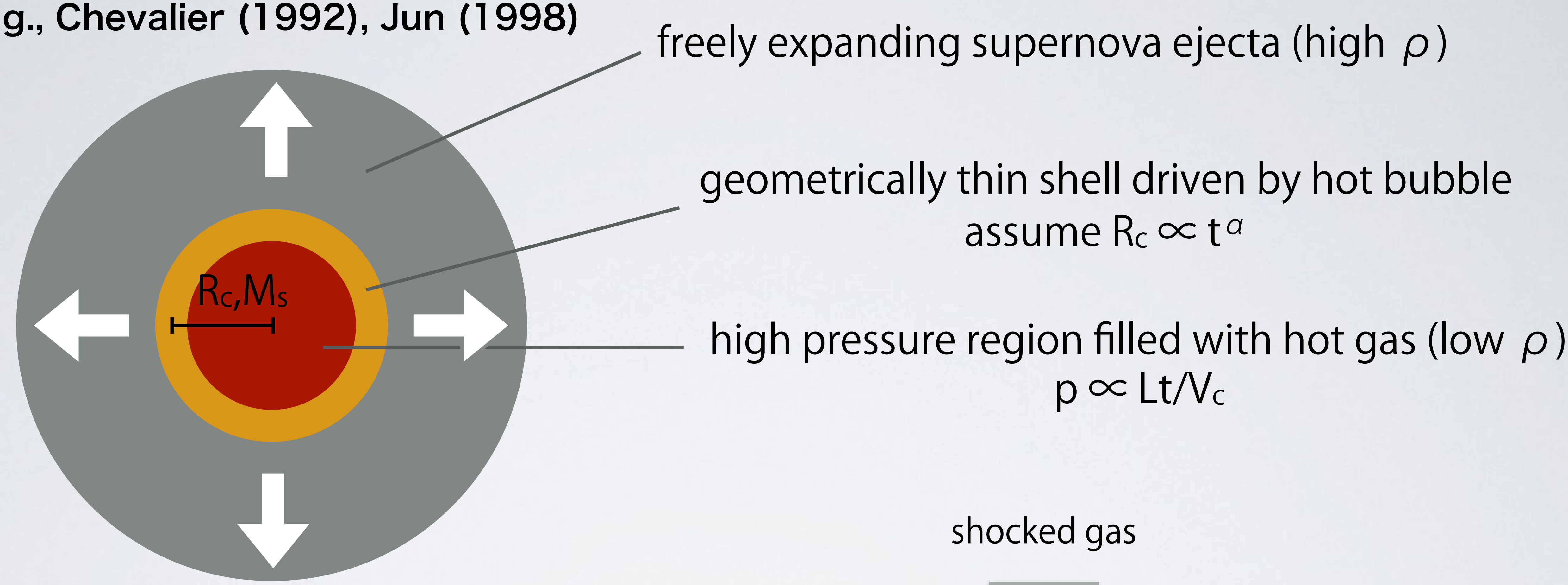

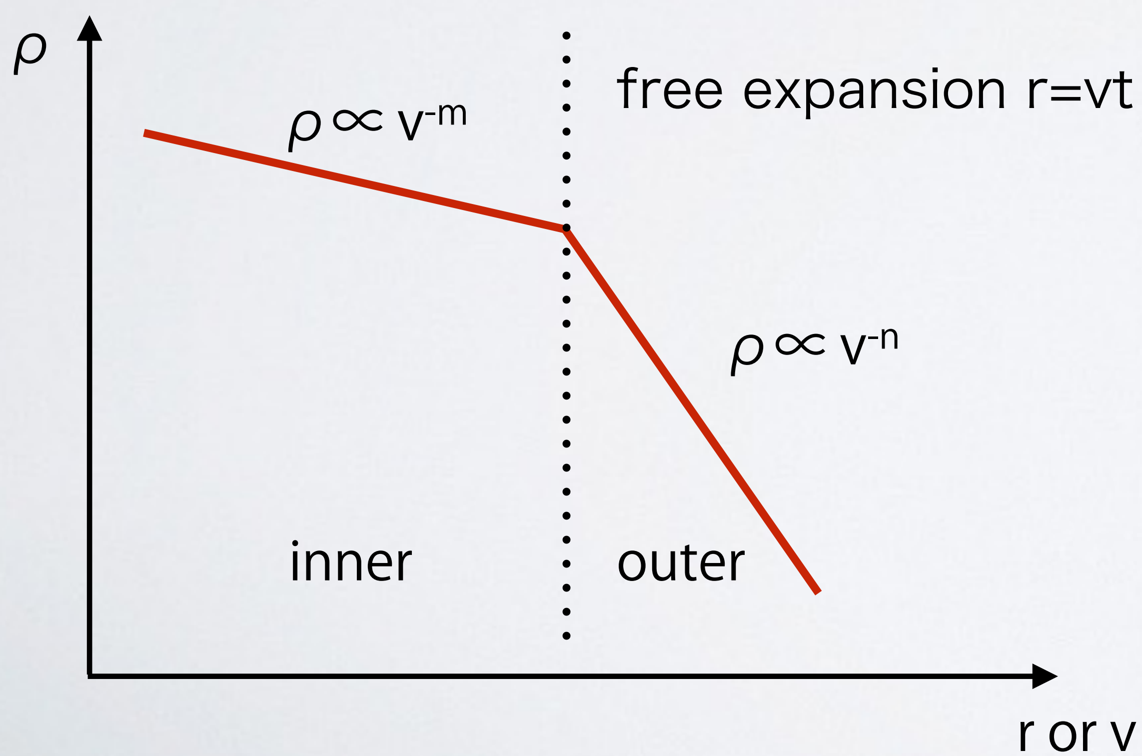

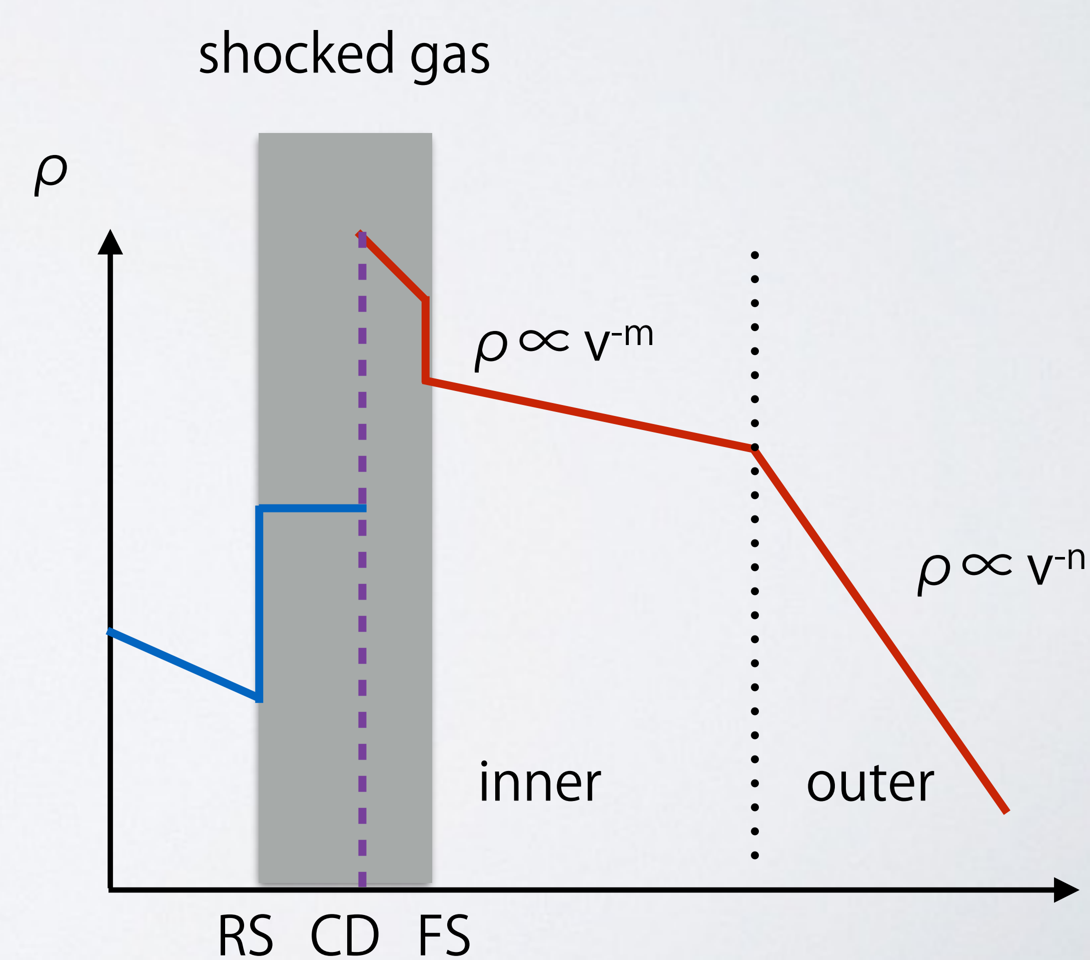

1D analytic model

e.g., Chevalier (1992), Jun (1998)

pressure of the hot bubble

$$p_c = \frac{3(\gamma-1)E_{\rm th}}{4\pi R_c^3} = \frac{3(\gamma-1)(2-\gamma)}{1+3\alpha(\gamma-1)} \frac{Lt}{4\pi R_c^3}$$

Eq. of continuity

$$M(t) \propto \int_0^r \rho(t,r) r^2 dr \propto t^{m-3} r^{3-m}$$

Eq. of motion

$$M(t)\frac{d^2 R_c}{dt^2} = 4\pi R_c^2 p_c \propto \frac{t}{R_c}$$

$$R_c^{5-m} \propto t^{6-m} \quad \Rightarrow \quad R_c \propto t^{\alpha}, \quad \text{with } \alpha = \frac{6-m}{5-m}$$

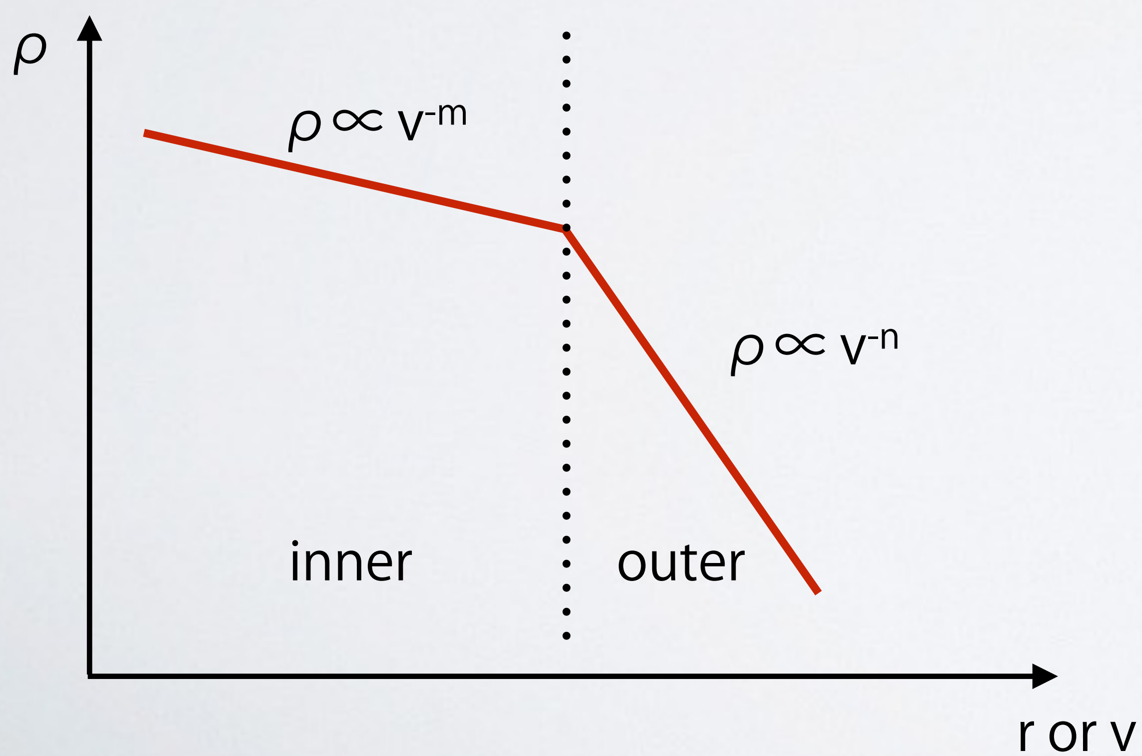

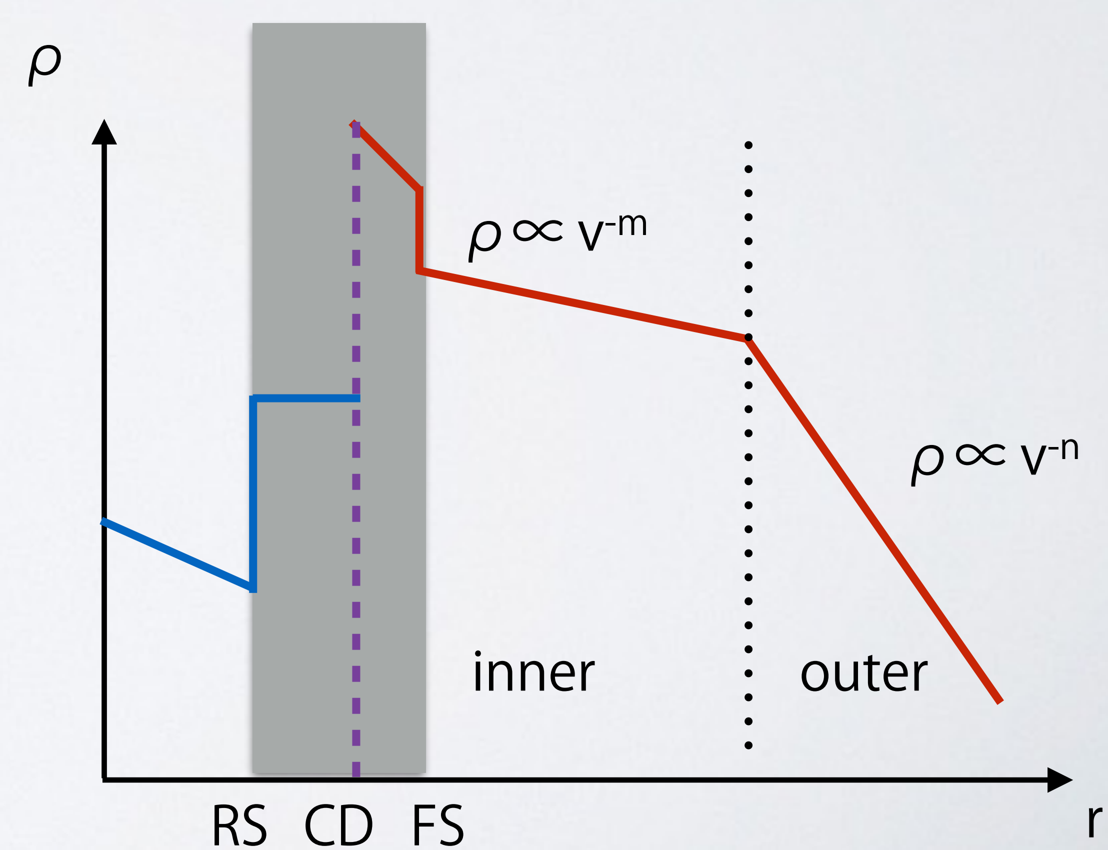

1D spherical picture of SN-wind interaction

- In 1D spherical case, the energy redistribution is realized by a geometrically thin shell (swept up materials by the energy injection) and the radiation diffusing out from the shell.
- It seems OK to explain the high brightness of SLSNe.

1D RHD simulation by Kasen&Bildsten (2010)

geometrically thin shell

magnetar energy injection

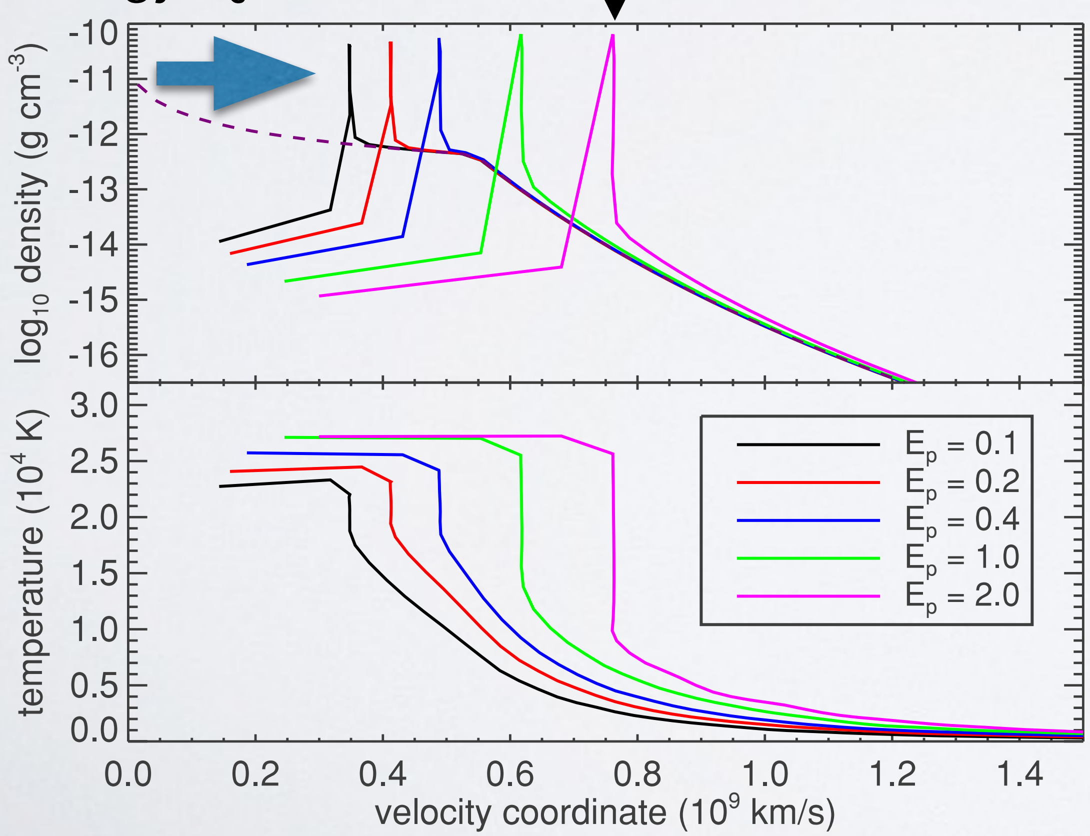

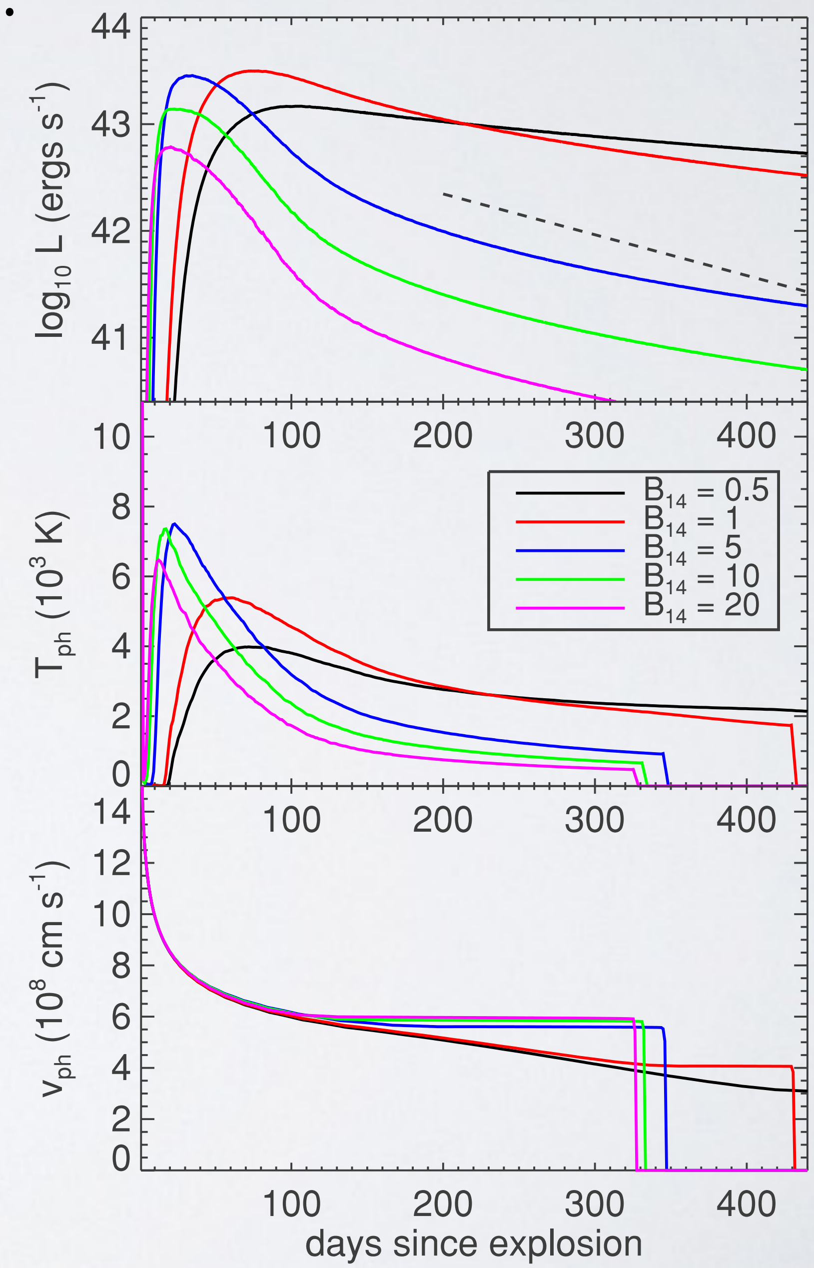

Q: Is 1D picture correct?

- No.
- From 1D analysis, we see that the shell is accelerating ($\alpha > 1$)
- an accelerating spherical shell is Rayleigh-Taylor unstable!
- more precisely, the unstable condition is “(dp/dr) x (d ρ /dr) <0”

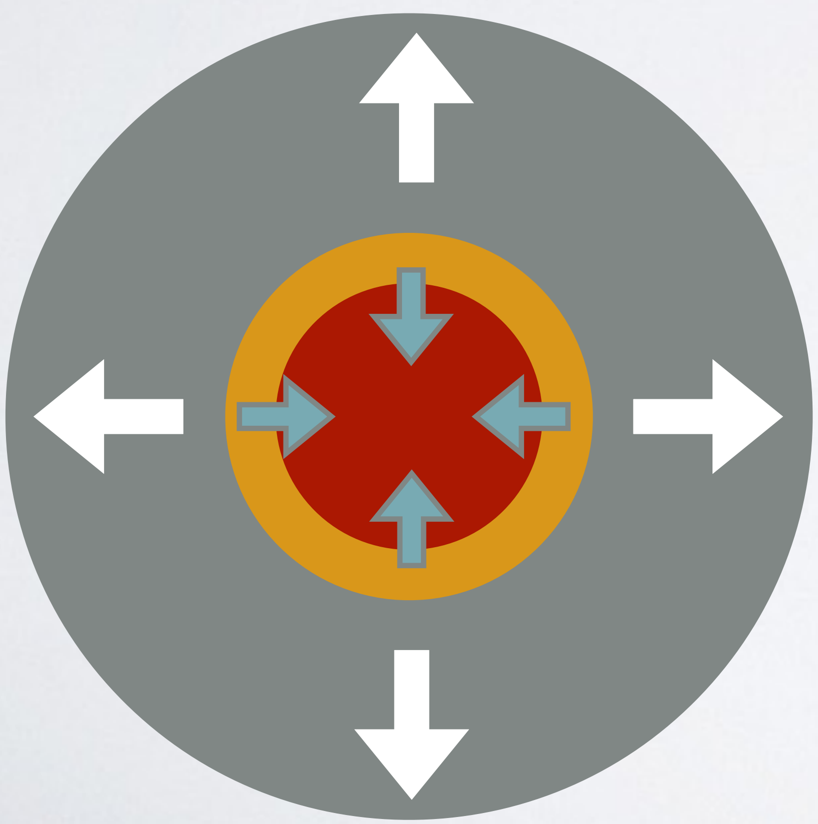

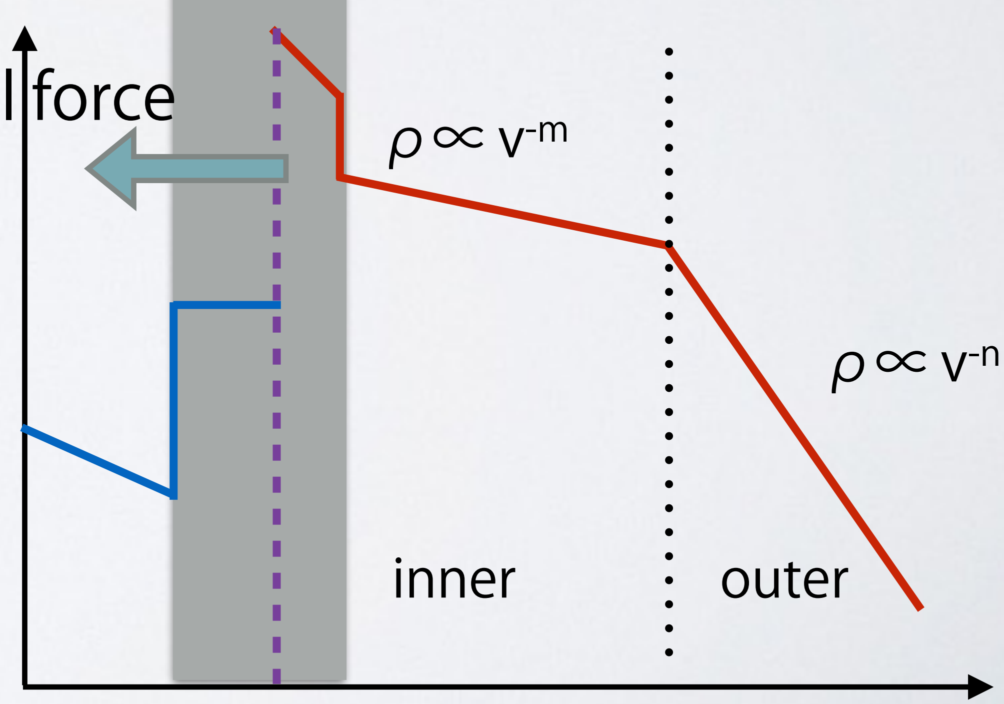

Q: Energy Redistribution in the Ejecta

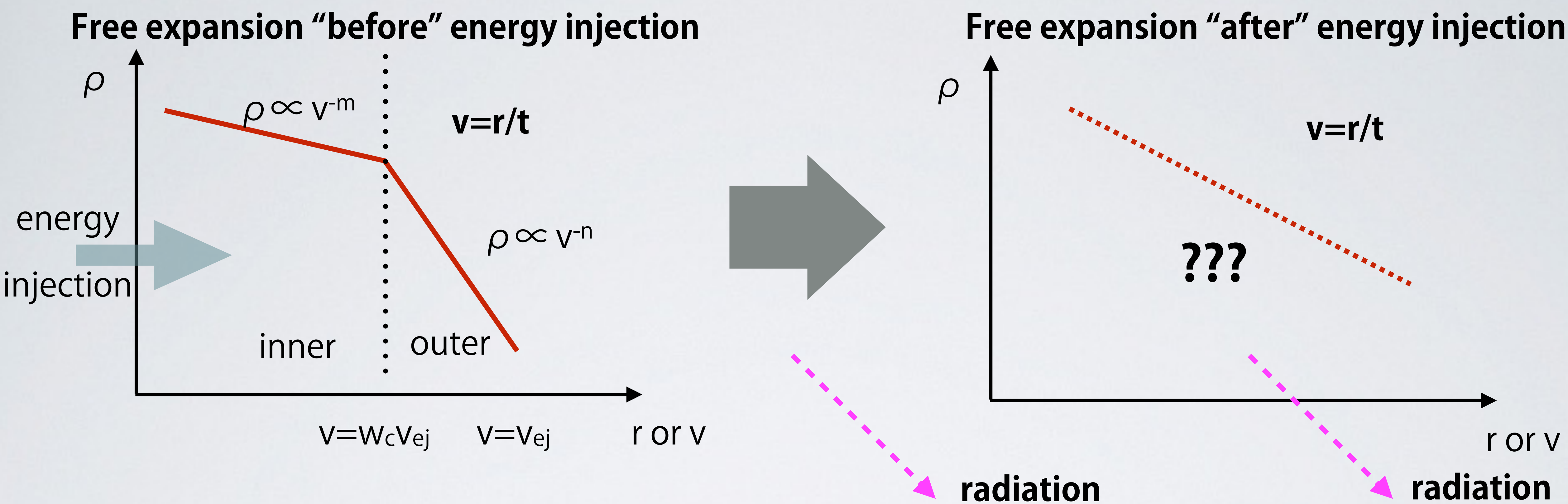

- We can inject relativistic flow from the central engine into SN ejecta in an analogy to PWNe.
- How the injected energy is **transferred** and **redistributed** in the SN ejecta?
- What is the **density and energy distributions of the SN ejecta** after being powered by the additional energy injection?
- How efficiently the injected energy can be converted to radiation escaping the ejecta (**radiation efficiency**)?

2D simulation (Suzuki&Maeda 2017)

- cylindrical coordinate (r,z)
- r,z in [0,1.2x10^{16} cm]x[-1.2x10^{16} cm,1.2x10^{16} cm]
- AMR technique. effective cell number 32,768 x 65,536
- ideal gas law γ =4/3
- relativistic gas injection within 3x10^{12} [cm] : L=10^{46} [erg/s] up to 10^{52} [erg]
- dM/dt=0.05L/c^2
- SN ejecta with 10[M$_\odot$] and 10^{51} [erg]
- unit time t_c=E_{sn}/L = 10^5sec
- from t=0.1t_c up to t=20.0t_c

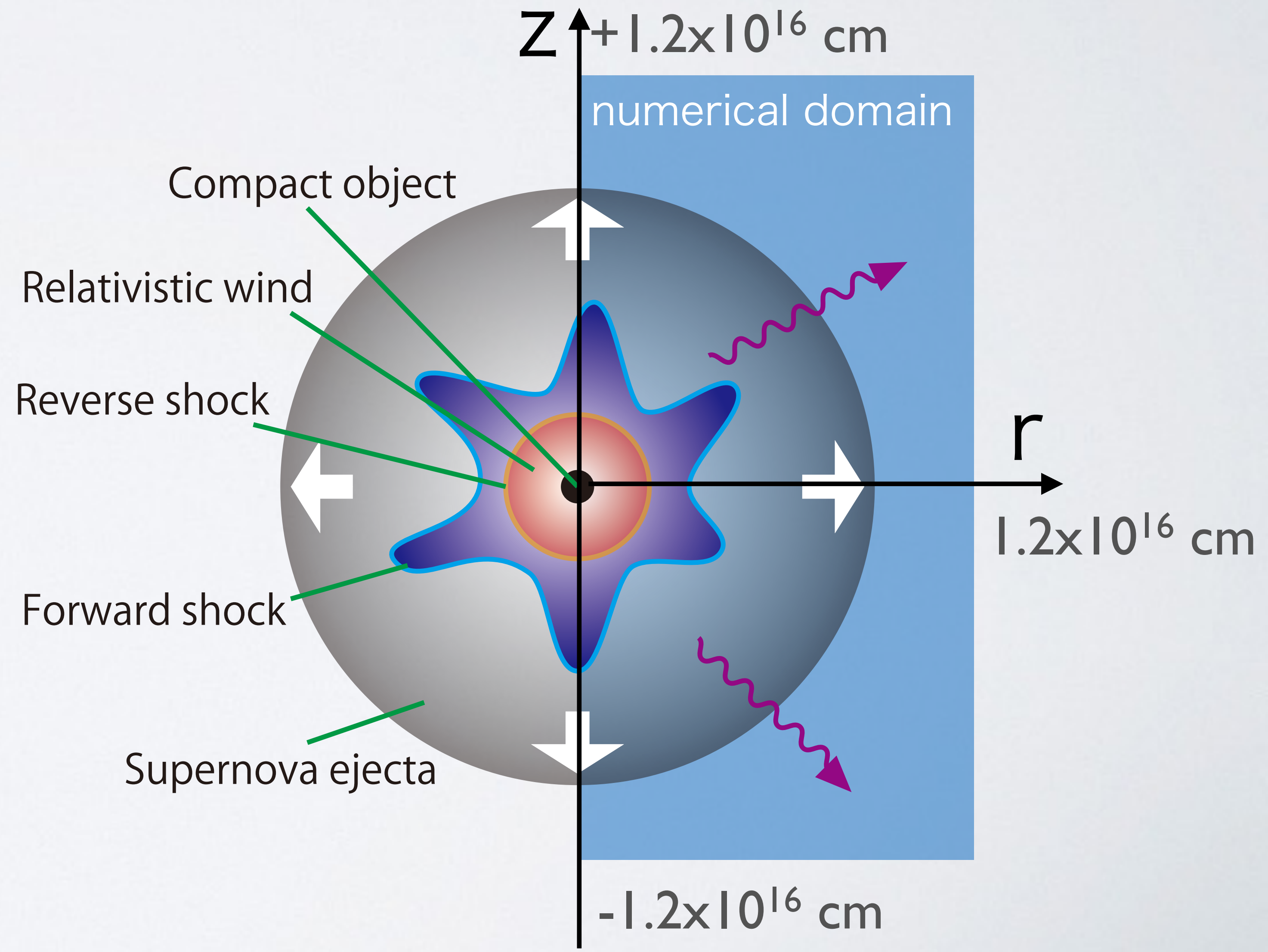

2D simulation (Suzuki&Maeda 2017)

- cylindrical coordinate (r,z)
- r,z in [0,1.2x10^{16} cm]x[-1.2x10^{16} cm,1.2x10^{16} cm]
- AMR technique. effective cell number 32,768 x 65,536
- ideal gas law γ =4/3
- relativistic gas injection within 3x10^{12} [cm] : L=10^{46} [erg/s] up to 10^{52} [erg]
- dM/dt=0.05L/c^2
- SN ejecta with 10[$M_\odot$] and 10^{51} [erg]
- unit time t_c=E_{sn}/L = 10^5sec
- from t=0.1t_c up to t=20.0t_c

E_{SN}=10^{51}[erg], M_{ej}=10[$M_\odot$]

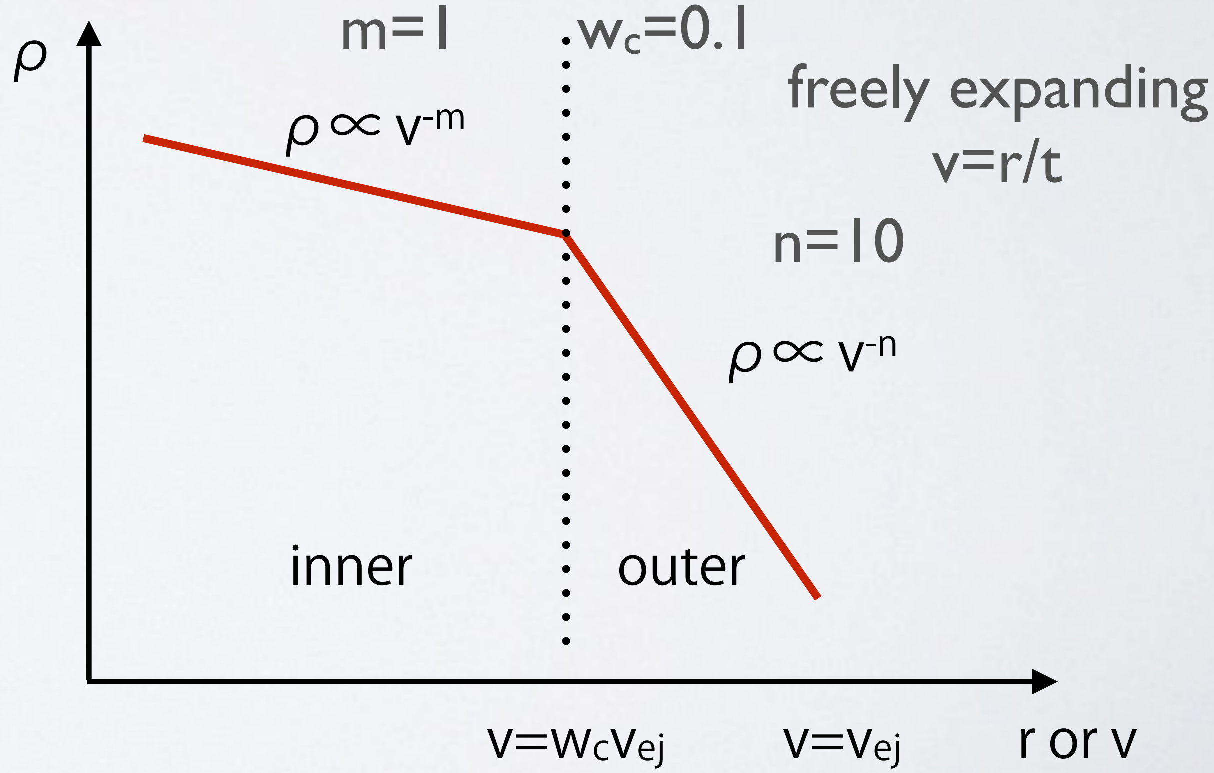

2D simulation (Suzuki&Maeda 2017)

- cylindrical coordinate (r,z)
- r,z in [0,1.2x10^{16} cm]x[-1.2x10^{16} cm,1.2x10^{16} cm]
- AMR technique. effective cell number 32,768 x 65,536
- ideal gas law γ =4/3
- relativistic gas injection within 3x10^{12} [cm] : L=10^{46} [erg/s] up to 10^{52} [erg]
- dM/dt=0.05L/c^2
- SN ejecta with 10[$M_\odot$] and 10^{51} [erg]
- unit time $t_c=E_{sn}/L$ = 10^5sec
- from t=0.1t_c up to t=20.0t_c

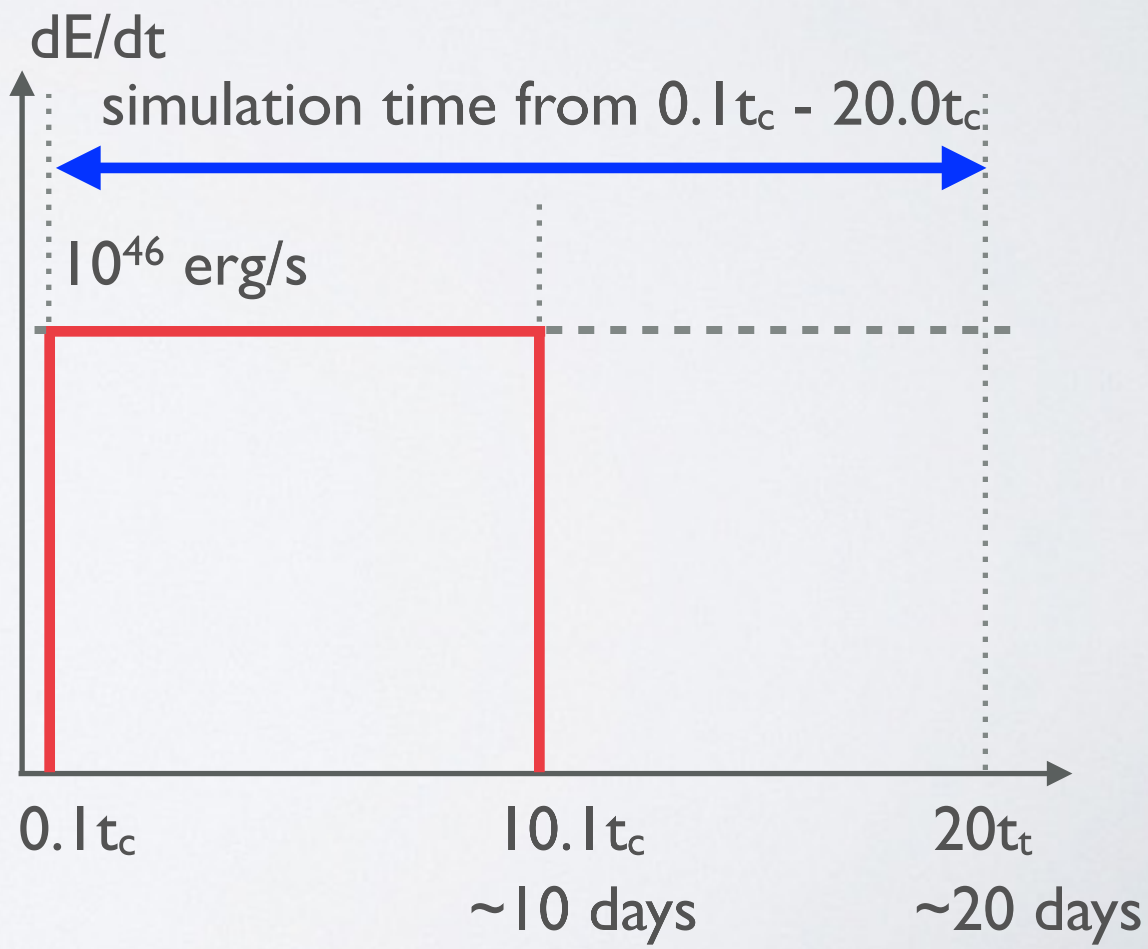

2D simulation (Suzuki&Maeda 2017)

$E_{sn}=10^{51}$ [erg], $L=10^{46}$ [erg/s], $t_c=10^5$ [sec]

- Lorentz factor
- density
- pressure

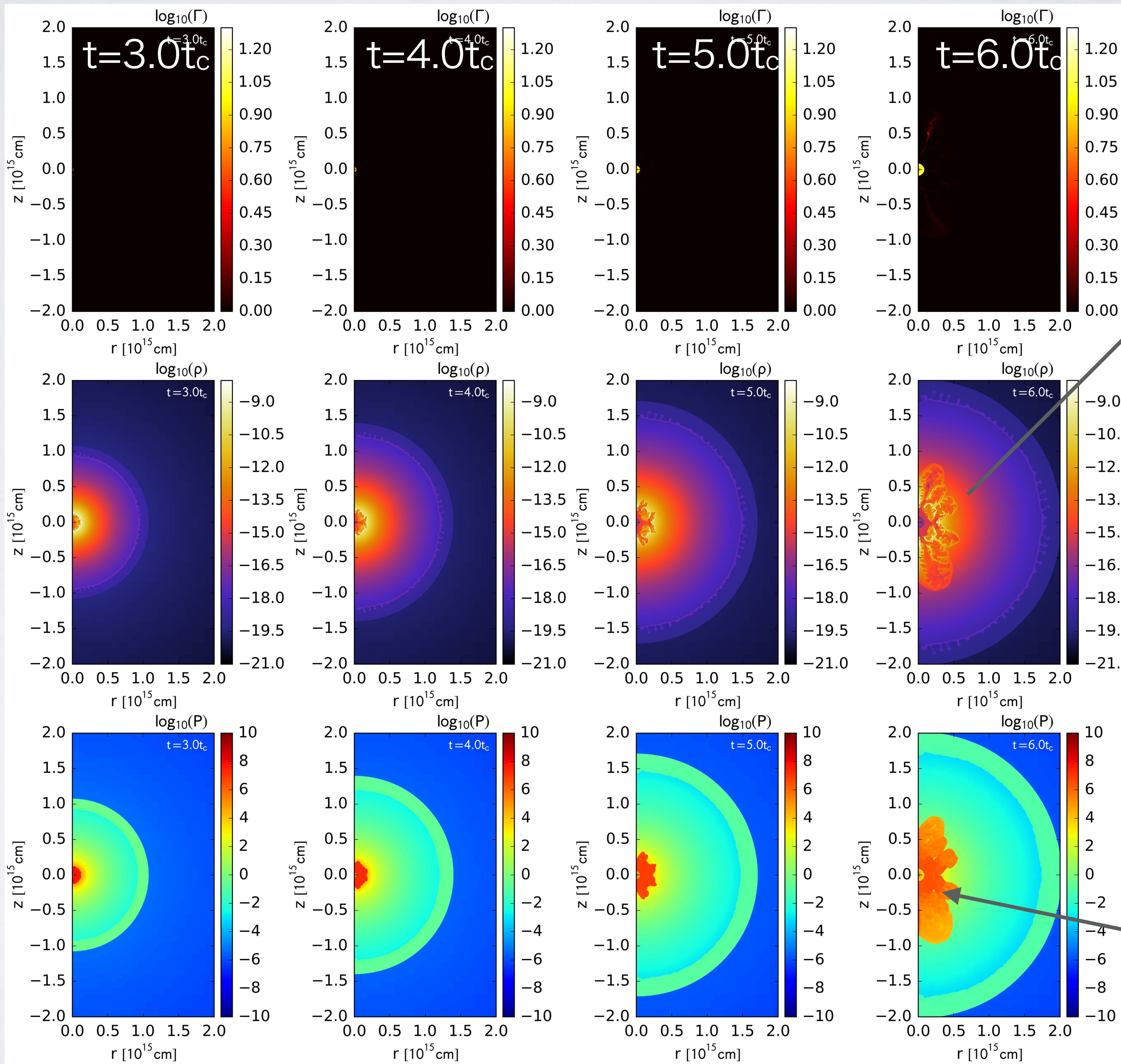

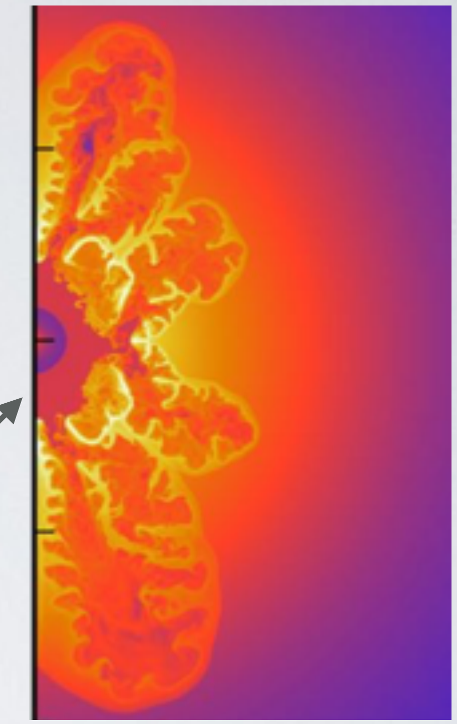

RT instability at the contact discontinuity

hot bubble powered by the central engine

2D simulation (Suzuki&Maeda 2017)

Clumpy density structure as a result of the energy injection

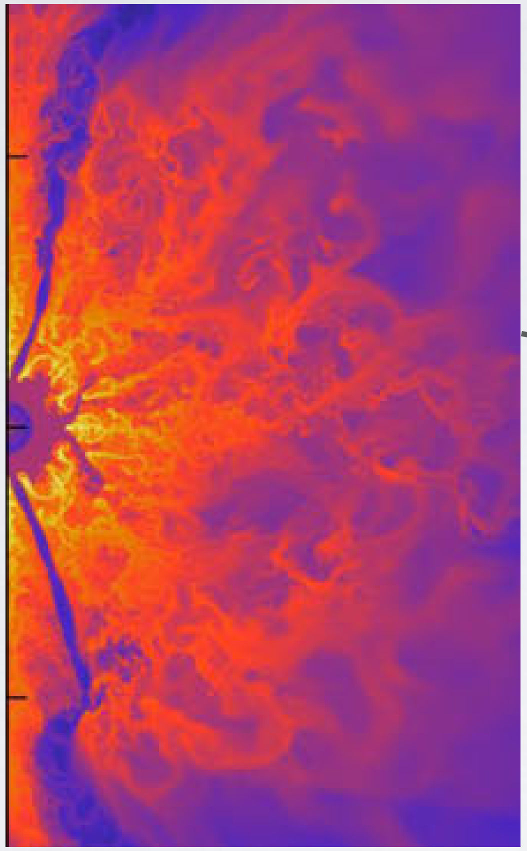

$E_{sn}=10^{51}$ [erg], $L=10^{46}$ [erg/s], $t_c=10^5$ [sec]

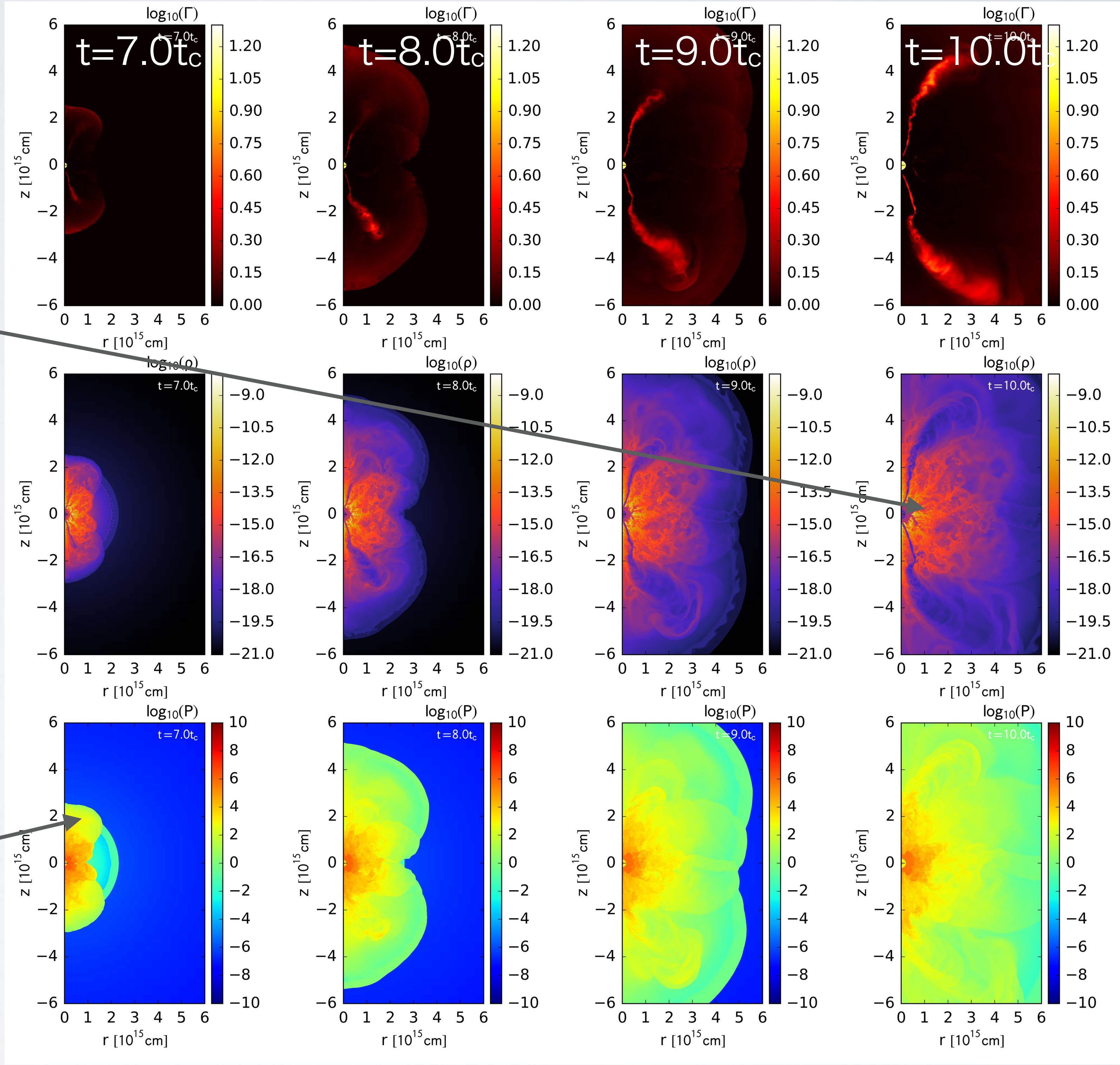

hot bubble inflation, leading to the breakout of the forward shock

Central engine model in 2D (Suzuki&Maeda2017)

- Lorentz factor
- density
- pressure

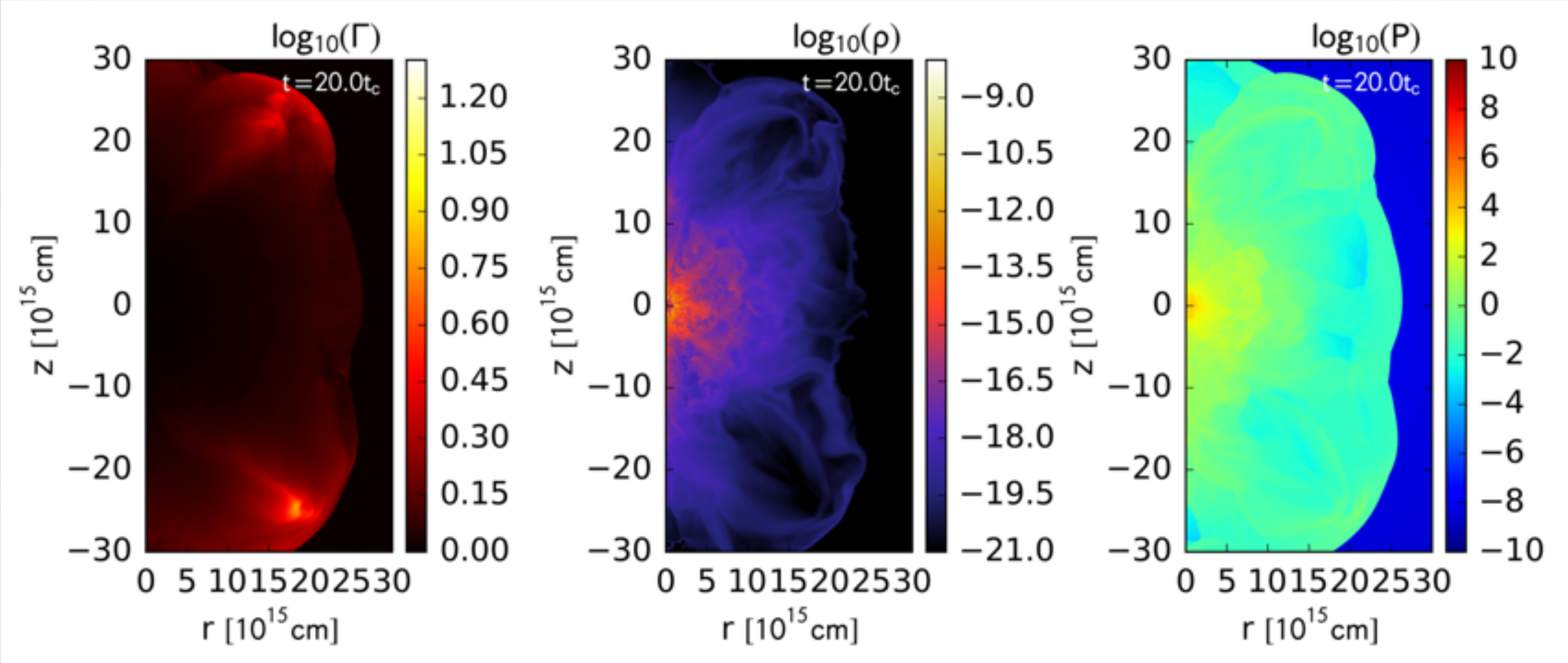

- The structure of the ejecta (almost) freely expanding after the energy injection (at ~ 20 days after explosion)
- The density structure is very complicated (clumpy, low-density channel)
- But, small-scale structure depends on the <u>numerical resolution</u>

Density distribution

Free expansion "before" energy injection

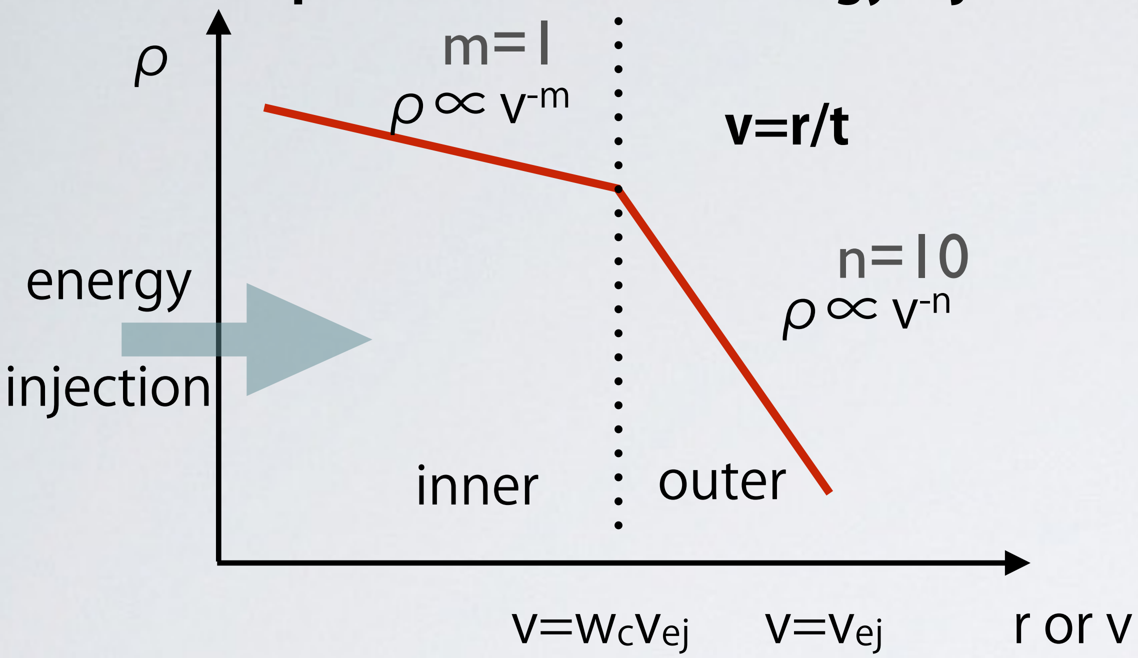

Free expansion "after" energy injection

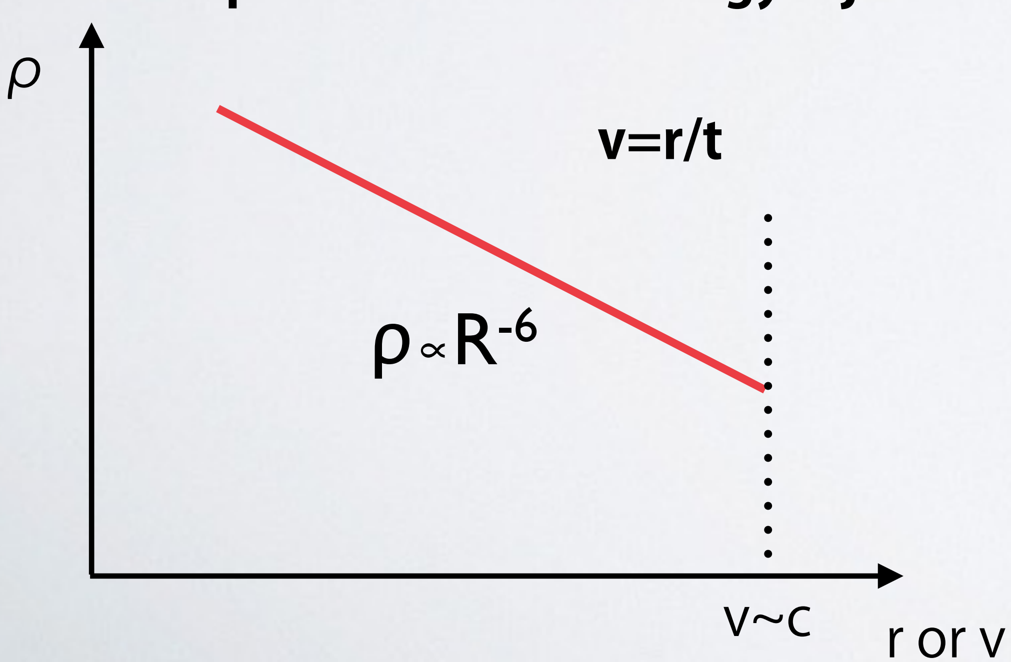

radial profiles at $t=20t_c$

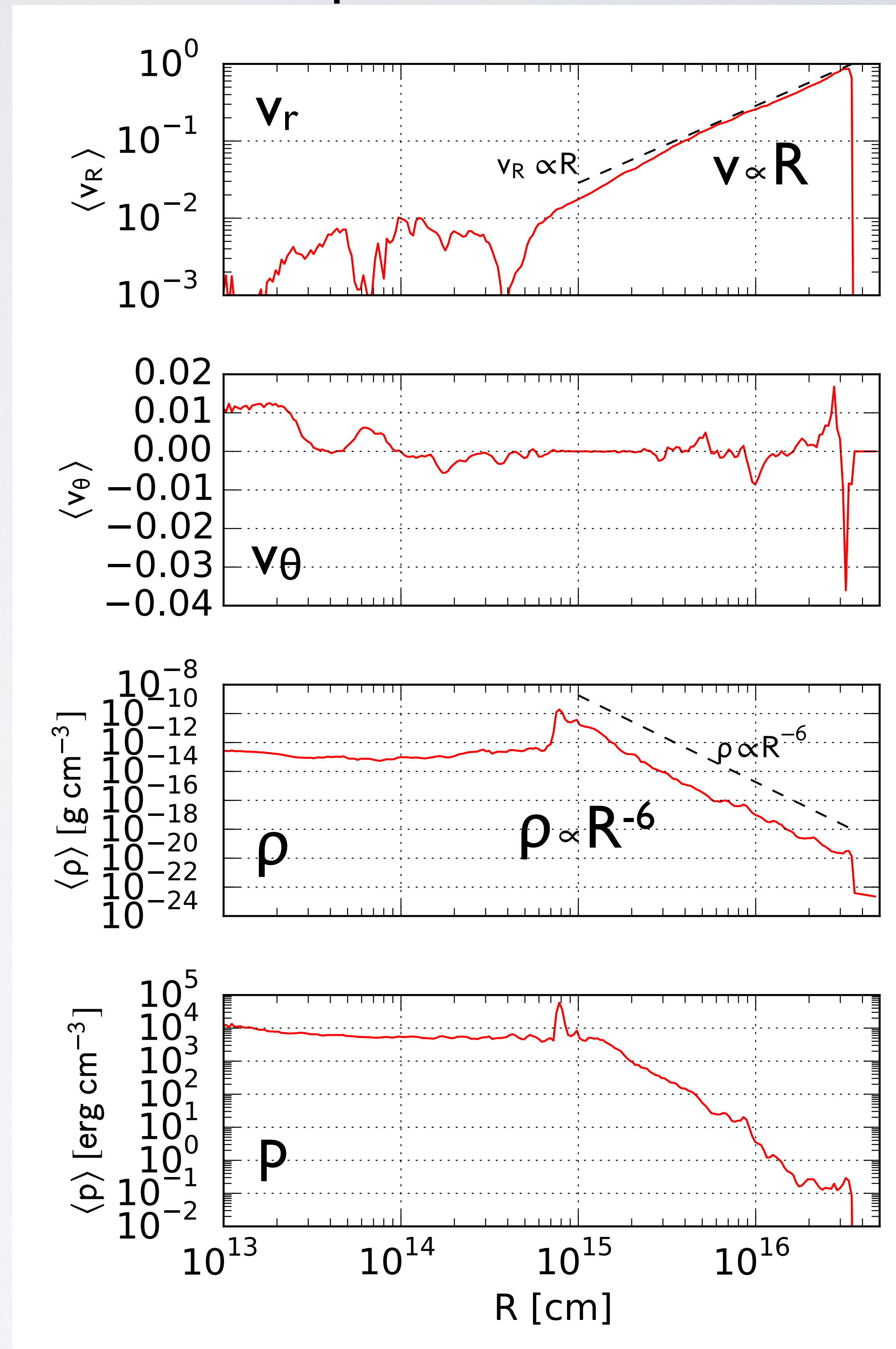

Density distribution

- density distribution realized for the flat energy spectrum
- kinetic luminosity at a radius is L: $4\pi R_0^2 \rho v^3 \propto L,$

  Note: R_0 is the radius of the Lagrange shell
  when the energy injection is completed ($t=10t_c$)

- We assume each Lagrangian shell travels at the velocity v
- We get

$$\rho(t, v) \propto \frac{L}{4\pi v^5 t^3} \frac{\mathrm{d}R_0}{\mathrm{d}v}.$$

- When $v \propto R_0$, the density obeys $\rho \propto v^{-5}$
- When $v \propto R_0^{\lambda}$ with $\lambda >> 1$, the density obeys $\rho \propto v^{-6}$
- Finally at the free expansion stage, we get a power-low density profile with an exponent from -5 to -6,
- The kinetic energy distribution is not completely flat, but the density distribution derived in this analysis it not that bad!

radial profiles at $t=20t_c$

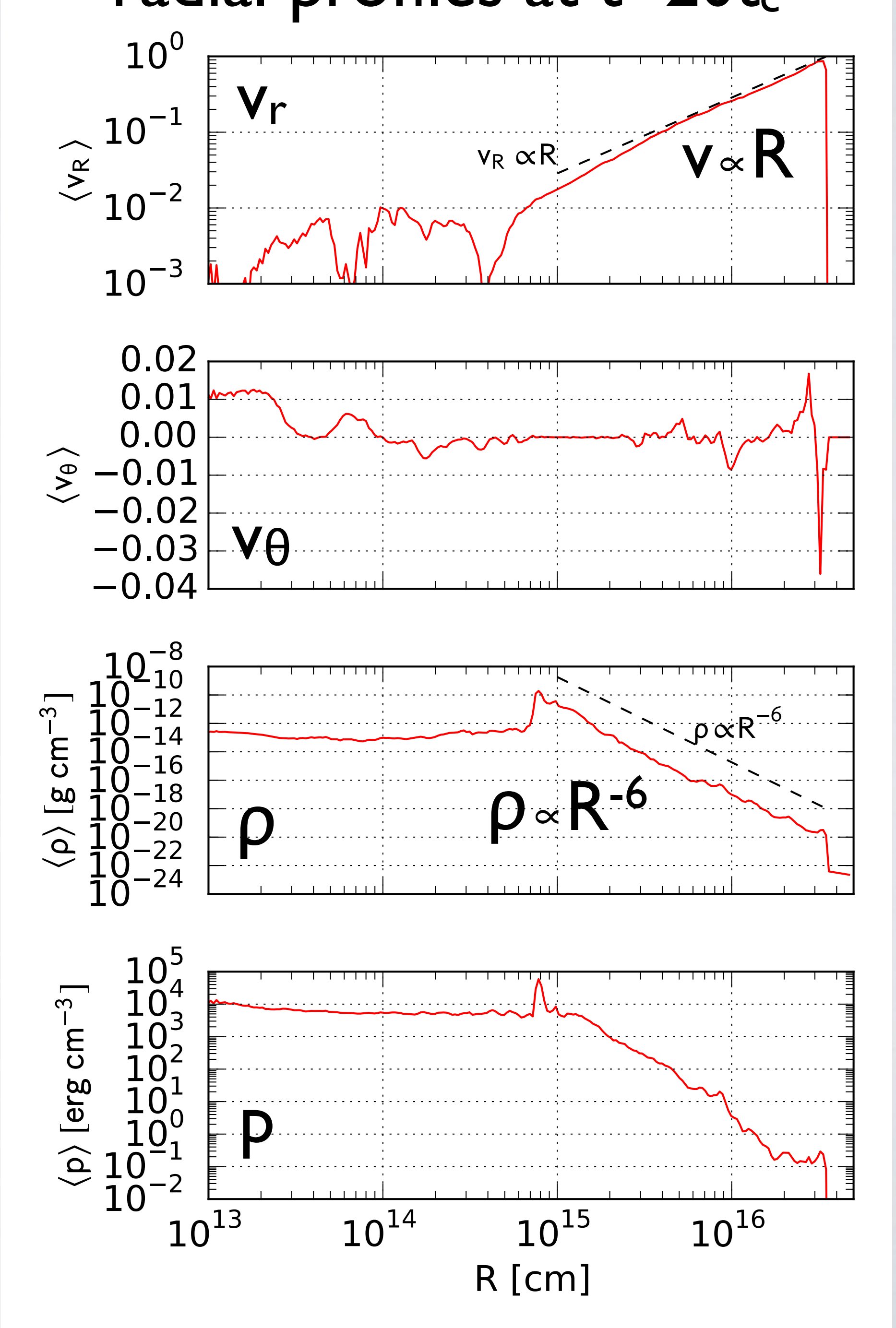

Density distribution

- density distribution realized for the flat energy spectrum
- kinetic luminosity at a radius is L: $4\pi R_0^2 \rho v^3 \propto L,$

  Note: R_0 is the radius of the Lagrange shell
  when the energy injection is completed ($t=10t_c$)
- We assume each Lagrangian shell travels at the velocity v
- We get

$$\rho(t, v) \propto \frac{L}{4\pi v^5 t^3} \frac{\mathrm{d}R_0}{\mathrm{d}v}.$$

- When $v \propto R_0$, the density obeys $\rho \propto v^{-5}$
- When $v \propto R_0{}^{\lambda}$ with $\lambda >> 1$, the density obeys $\rho \propto v^{-6}$
- Finally at the free expansion stage, we get a power-low density profile with an exponent from -5 to -6,
- The kinetic energy distribution is not completely flat, but the density distribution derived in this analysis it not that bad!

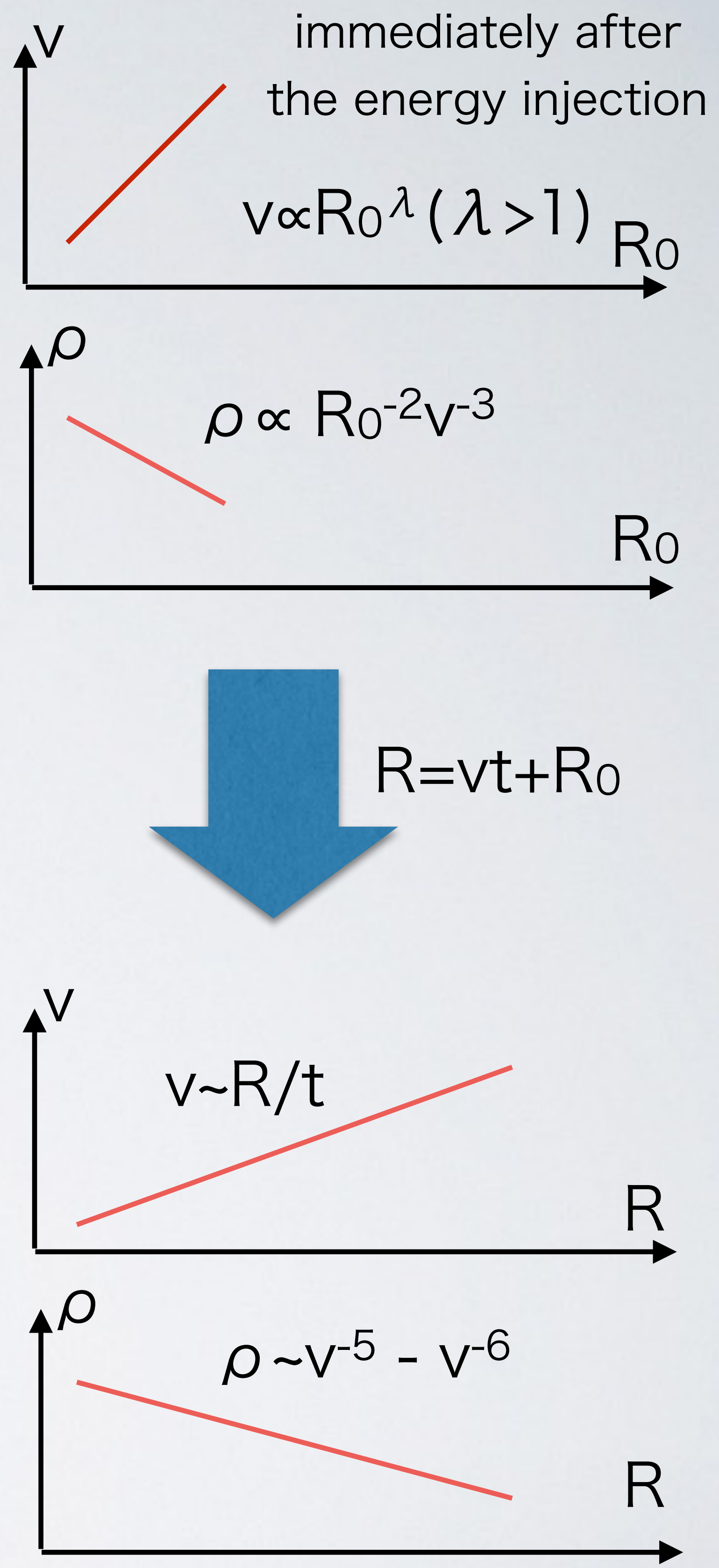

$$\rho(t, v) \propto \frac{L}{4\pi v^5 t^3} \frac{\mathrm{d}R_0}{\mathrm{d}v}.$$

Q: Is 2D simulation correct?

- Probably, no.
- In 2D simulation, we get "artificial" bipolar ejecta structure even when we assume spherical energy injection
- This is because of the presence of the symmetry axis
- 3D simulation with no assumed symmetry is needed!

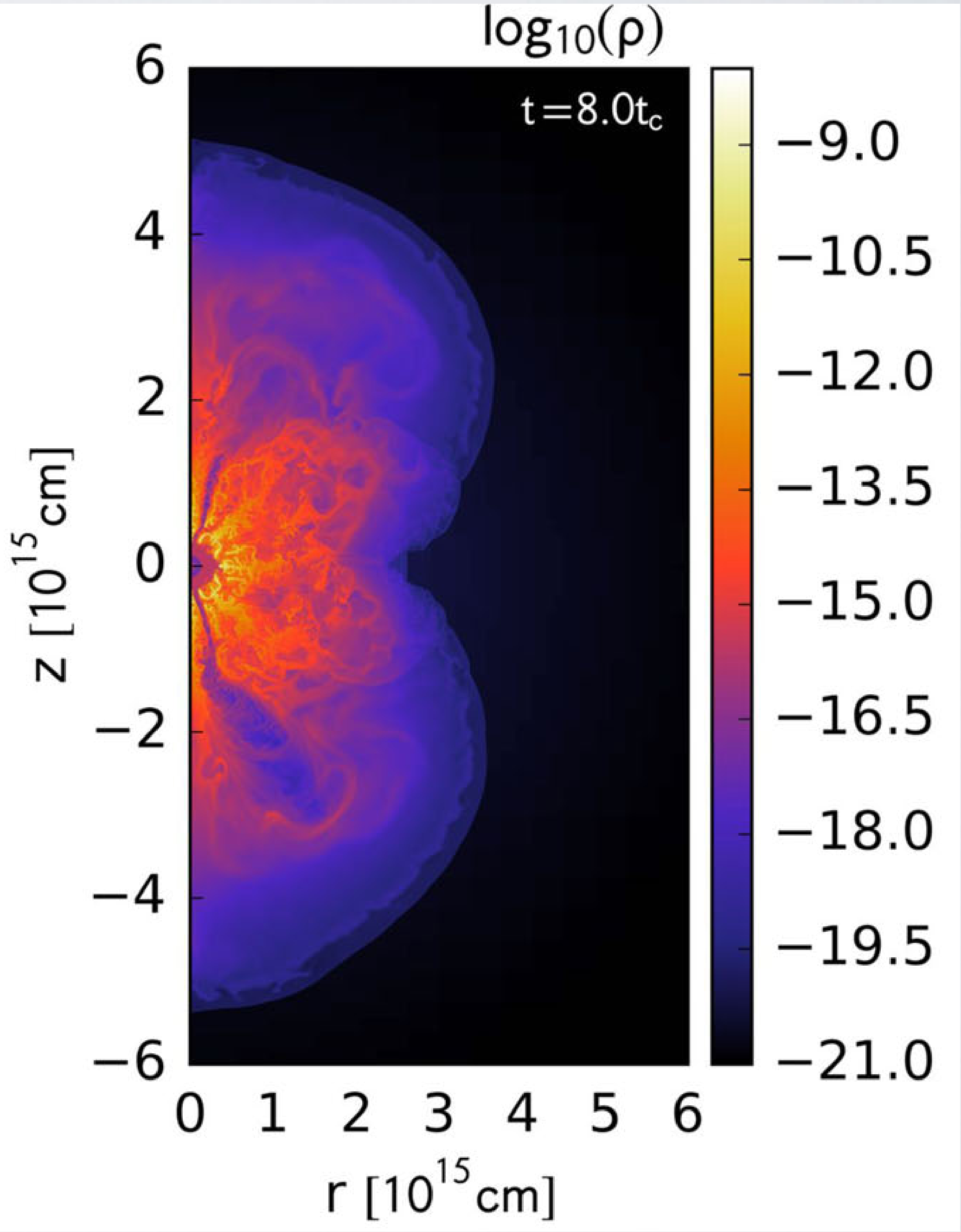

Summary: central-engine SNe in multi-D

- Dynamical evolution of SN ejecta + additional energy injection is multi-dimensional
- Hot bubble breakout leads to violent mixing
- final radial density structure of the ejecta is a simple power-law function
- we have started 3D simulations and confirmed the picture

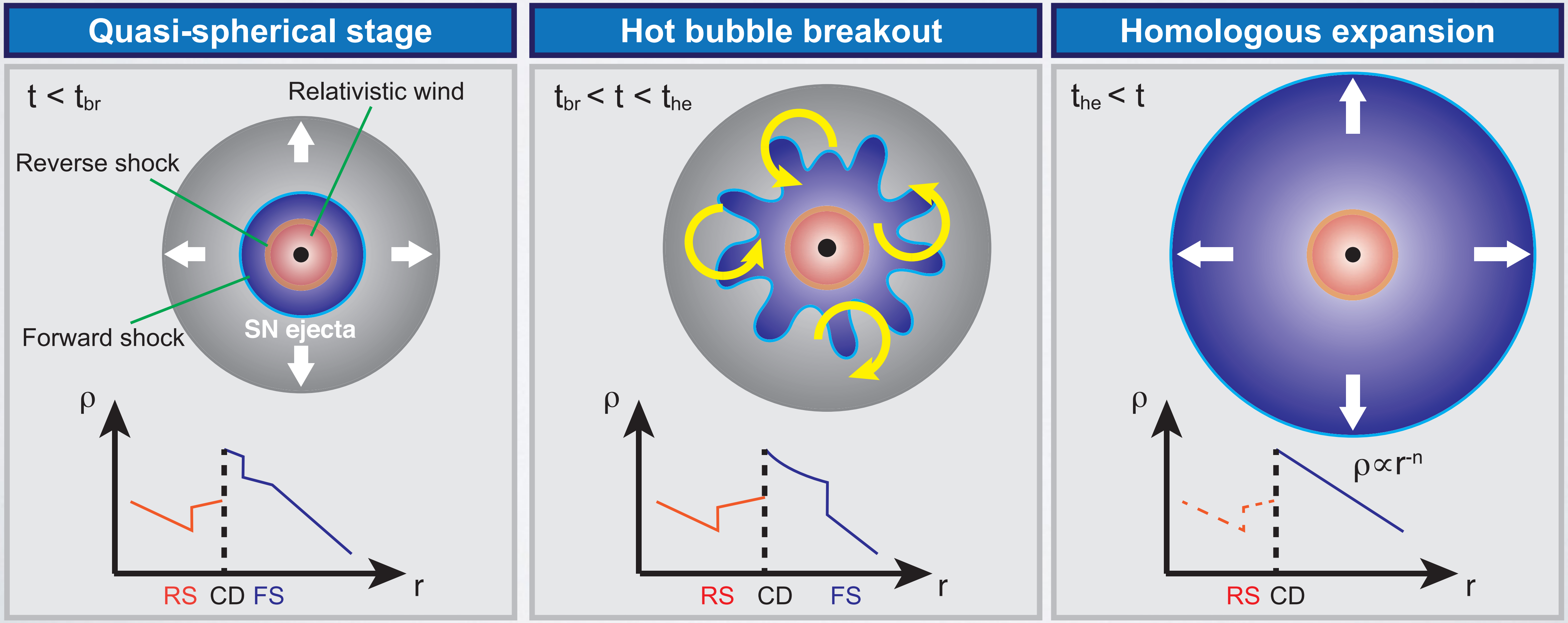

Future plans

- parameter surveys in 2D and 3D
- LC calculations by incorporating multi-D effect
- multi-band emission properties (including radio and X-ray)
- line transfer calculations to obtain theoretical spectrum of SLSNe

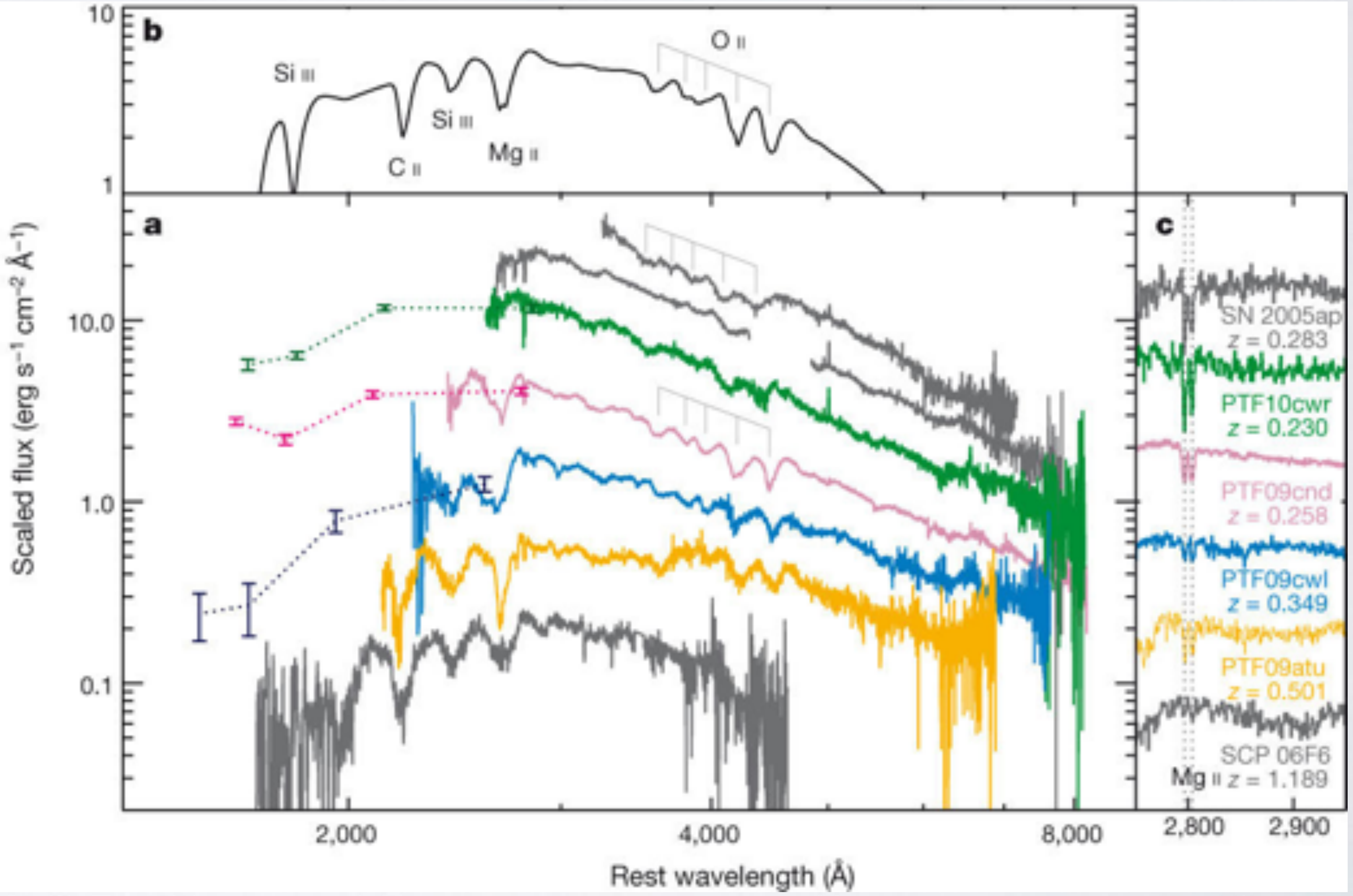

↑SLSNe-I spectra (Quimby+ 2011)

Backup slides

Ordinary and Extra-ordinary CCSNe

- CCSNe energetics: Canonically,
  - gravitational energy $E_{grav} \sim GM_{ns}^2/R_{ns} \sim$ **10^{53} [erg]**
  - kinetic energy $E_{kin} \sim$ **1%** of $E_{grav} \sim$ **10^{51} [erg]**
  - total radiated energy $E_{rad} \sim$ **less than 1%** of $E_{kin} \sim$ **$<10^{49}$ [erg]**
  - ejecta mass: **a few - 10 $M_\odot$**
  - photospheric velocity: typically, ~**10,000 [km/s]**

- However, some unusual SNe exceed these canonical numbers:
  - **broad-lined Ic SNe (Ic-BL)**: photospheric velocity larger by a factor of 2-3 ~ **20,000 [km/s]**, which implies $E_{kin} \sim$ **10^{52} [erg]** > 10^{51} [erg]
  - **Superluminous SNe (SLSNe)**: $E_{rad} \sim$ **10^{51} [erg]** > 10^{49} [erg]

This talk

Temporal evolution

- R_{peak}: the radius at which the gas show its peak density.
- E_{kin},E_{int}: kinetic and internal energies of the ejecta + relativistic gas
- their temporal evolutions show good agreement with analytical estimation until $t=t_{br}=5.1t_c$.
- After $t=t_{br}$, the internal energy of the gas saturates, suggesting that the energy of the bubble is leaking into the outer ejecta.

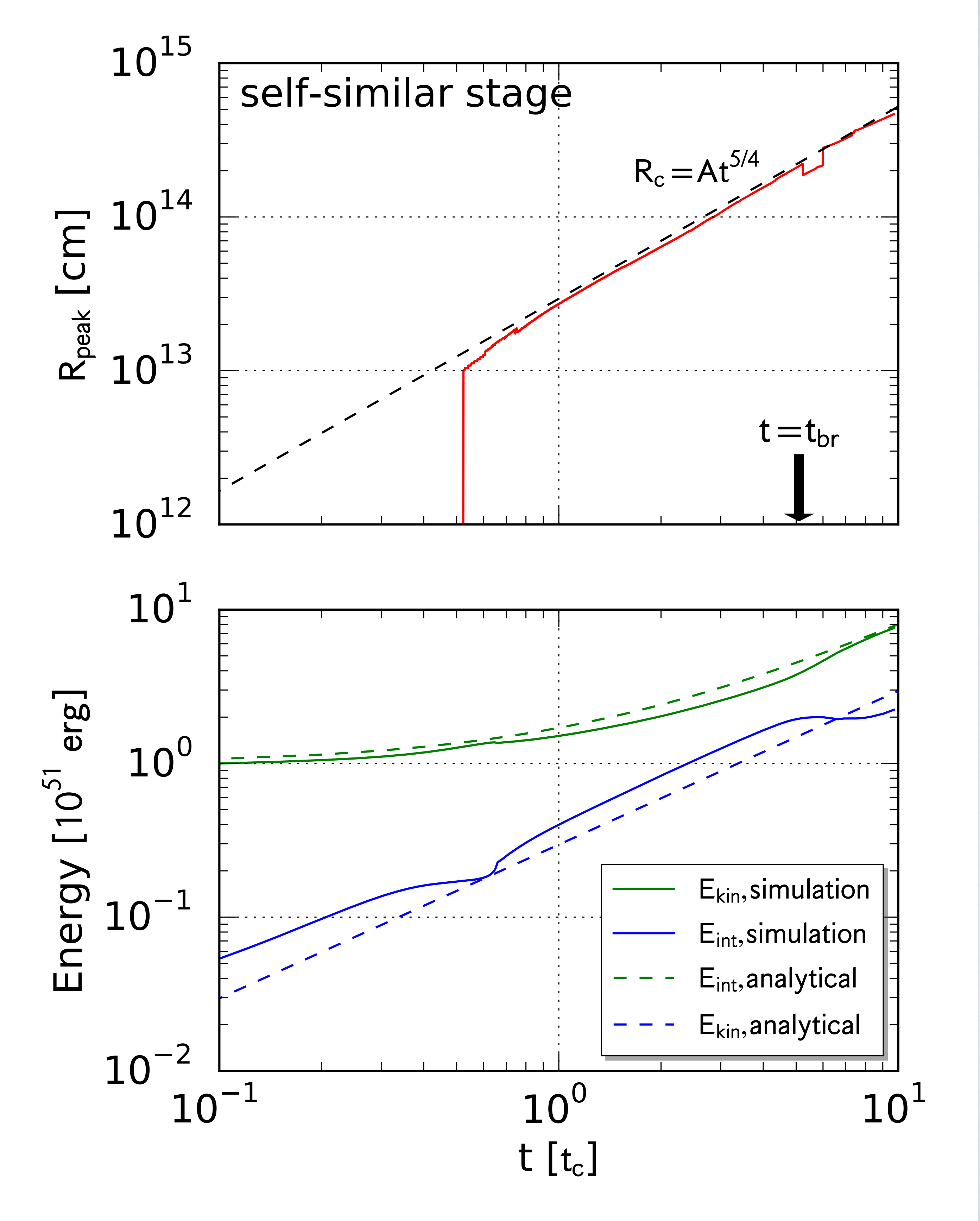

Central engine model in 2D (Suzuki&Maeda2017)

- angle-averaged density distribution at t~20 days after explosion
- ejecta are almost freely expanding: v∝R, up to v~c
- the density structure is well represented by a simple power-law function with an index -6

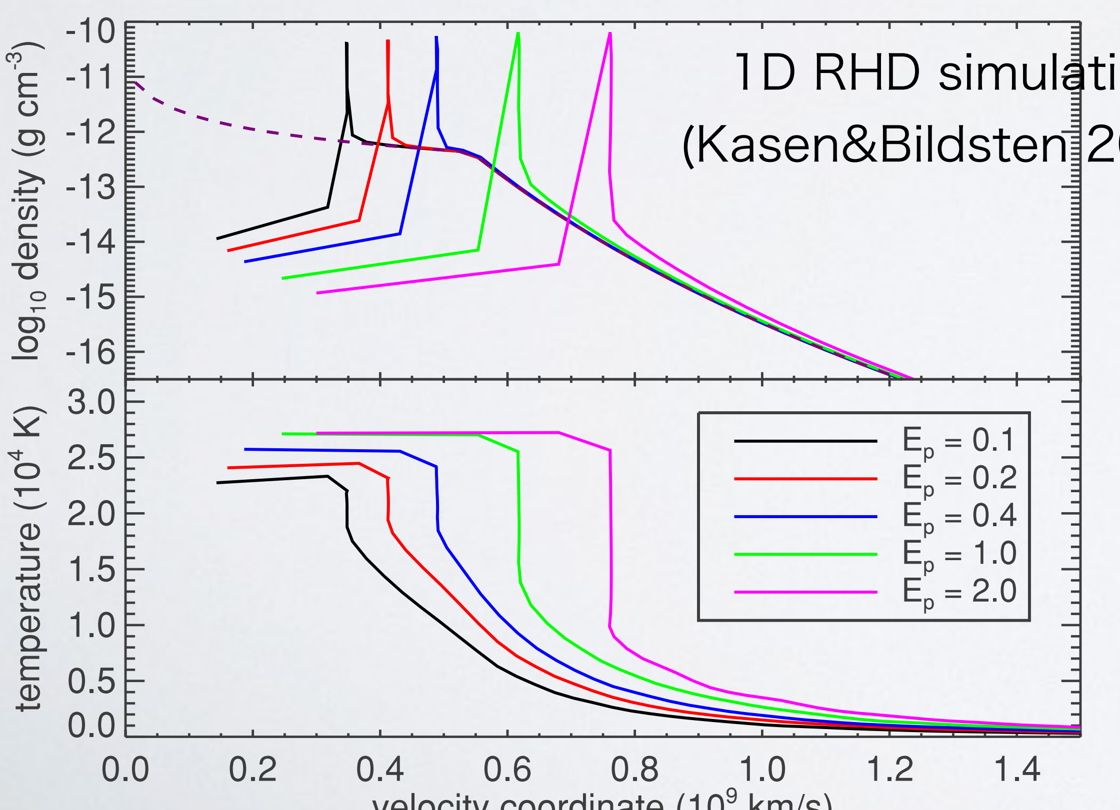

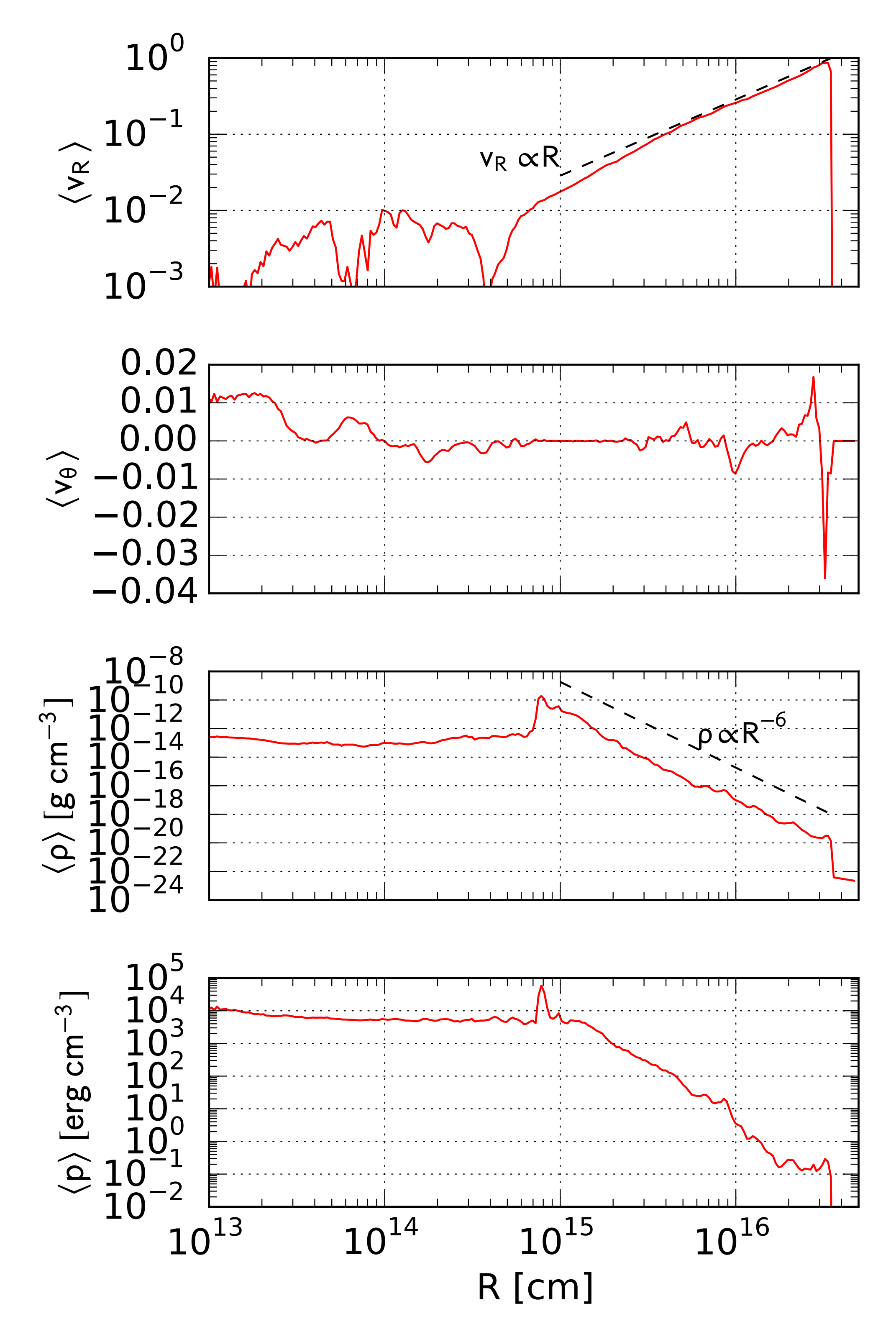

Density distribution

Free expansion “before” energy injection

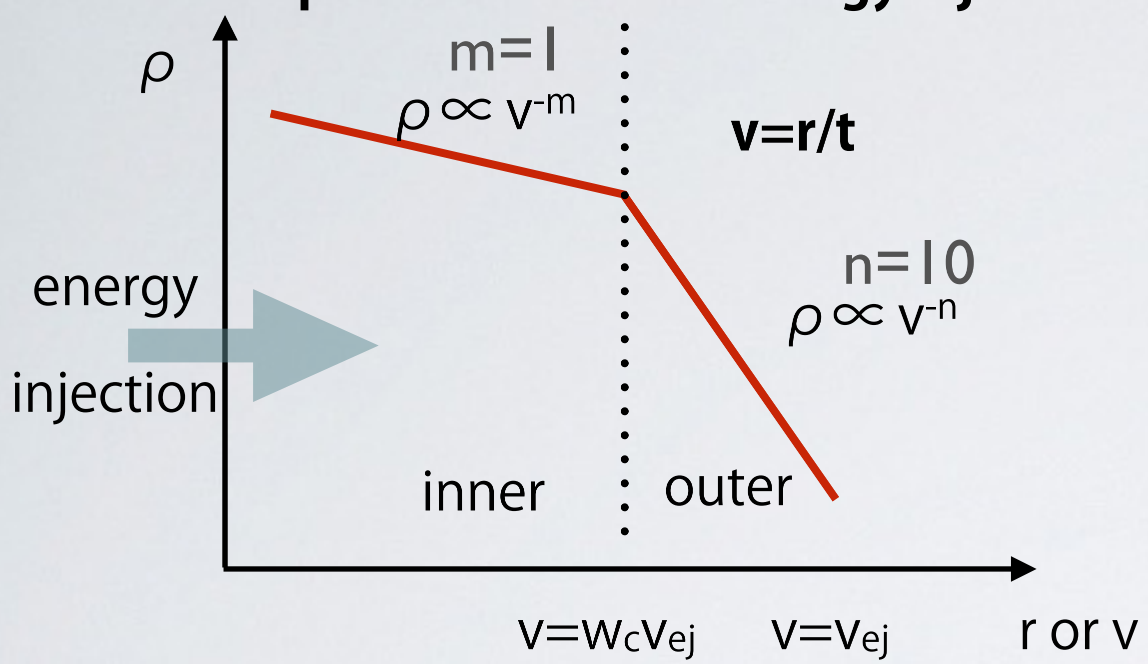

Free expansion “after” energy injection

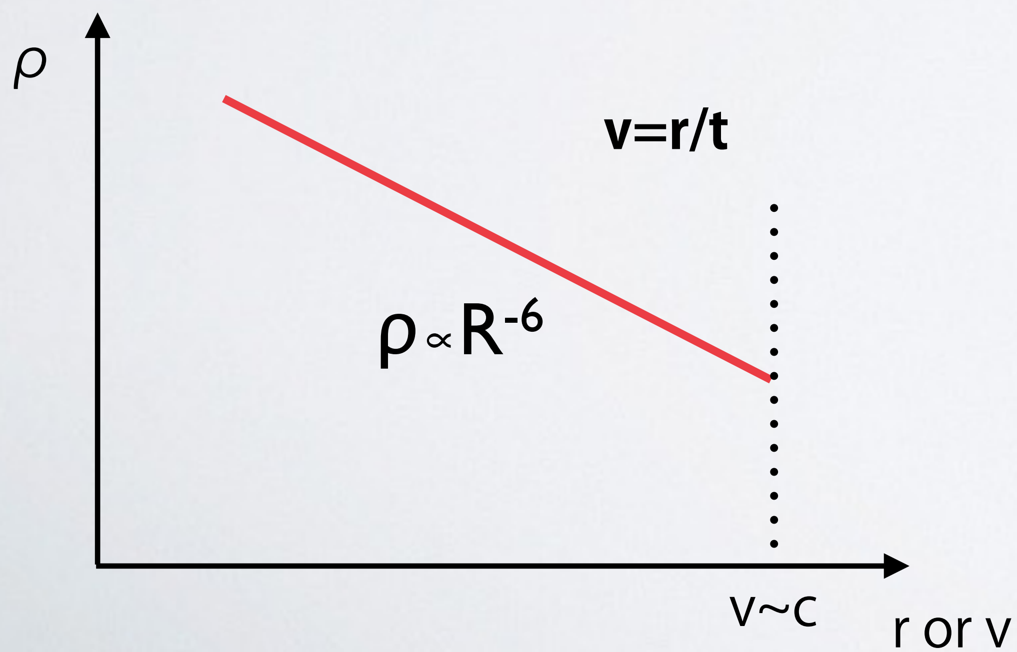

radial profiles at $t=20t_c$

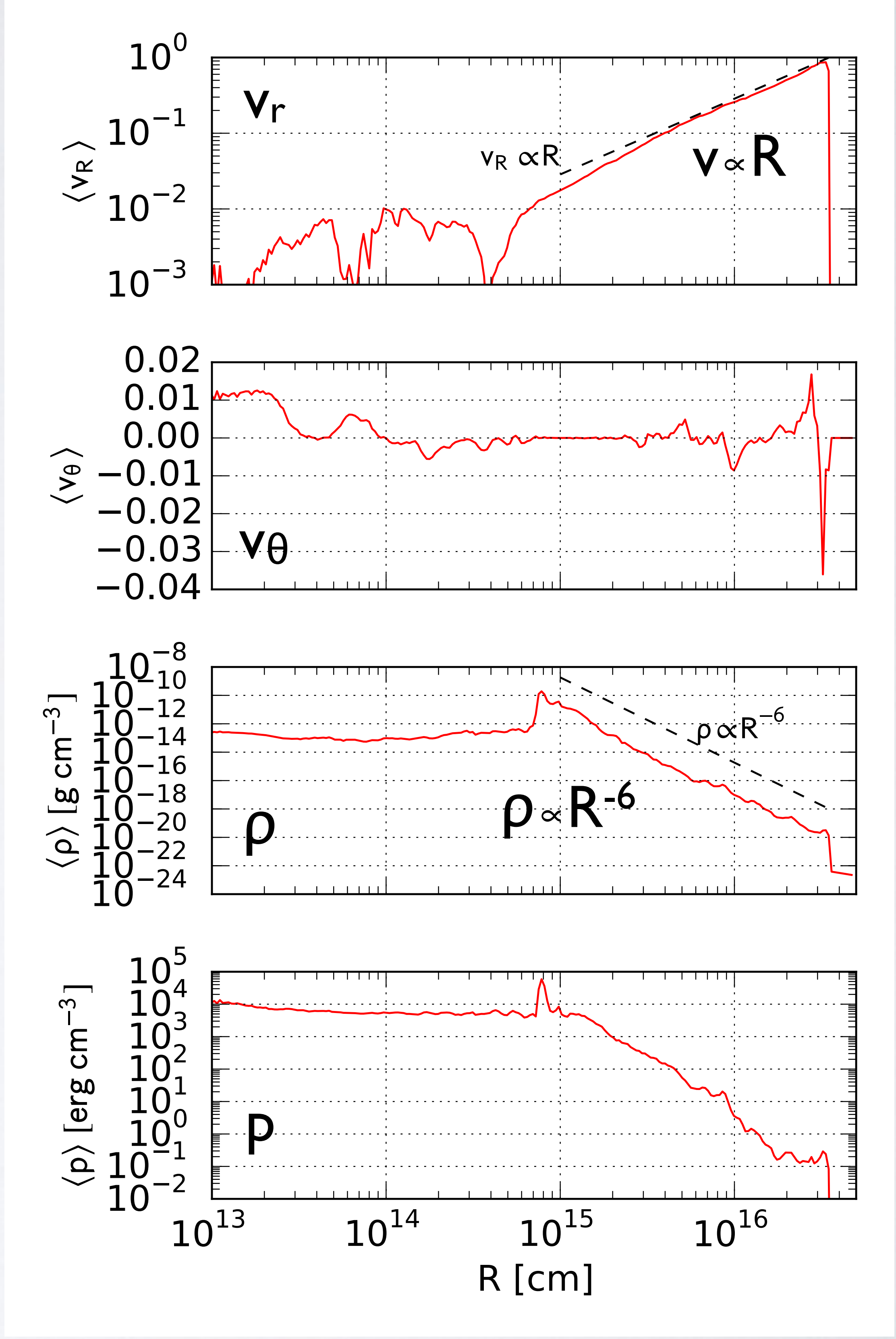

Energy Redistribution in the Ejecta

- In 1D spherical case, the outer layers are heated by diffusing photons.
- The situation in our multi-D simulation is qualitatively different.
- Gas flows emanating the hot bubble directly carry the injected energy to the outer layers of the ejecta → overall heating of the ejecta.

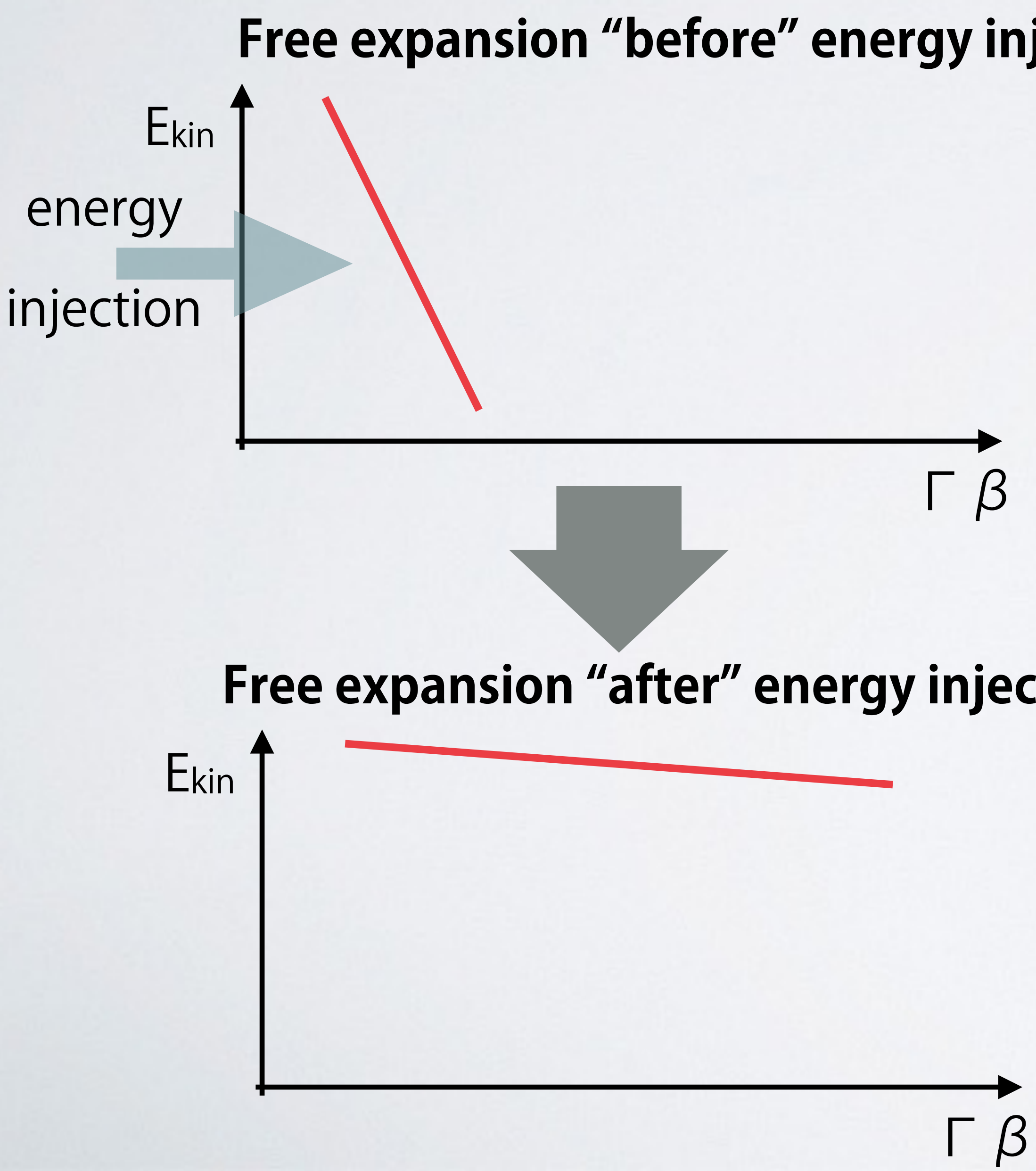

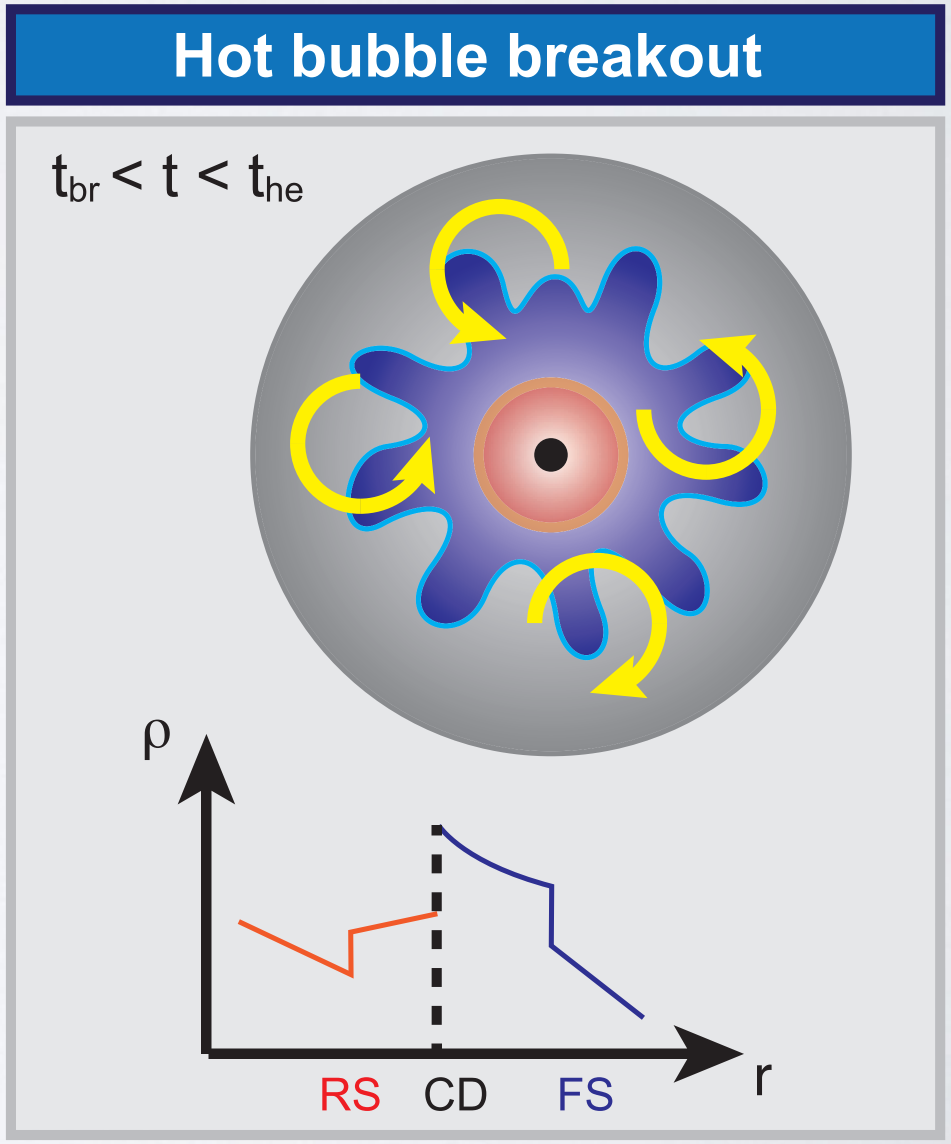

Density distribution

- density distribution realized for the flat energy spectrum
- kinetic luminosity at a radius is L: $4\pi R_0^2 \rho v^3 \propto L,$

  Note: R_0 is the radius of the Lagrange shell
  when the energy injection is completed ($t=10t_c$)

- We assume each Lagrangian shell travels at the velocity v
- We get

$$\rho(t, v) \propto \frac{L}{4\pi v^5 t^3} \frac{\mathrm{d}R_0}{\mathrm{d}v}.$$

- When $v \propto R_0$, the density obeys $\rho \propto v^{-5}$
- When $v \propto R_0^{\lambda}$ with $\lambda >> 1$, the density obeys $\rho \propto v^{-6}$
- Finally at the free expansion stage, we get a power-low density profile with an exponent from -5 to -6,
- The kinetic energy distribution is not completely flat, but the density distribution derived in this analysis it not that bad!

radial profiles at $t=20t_c$

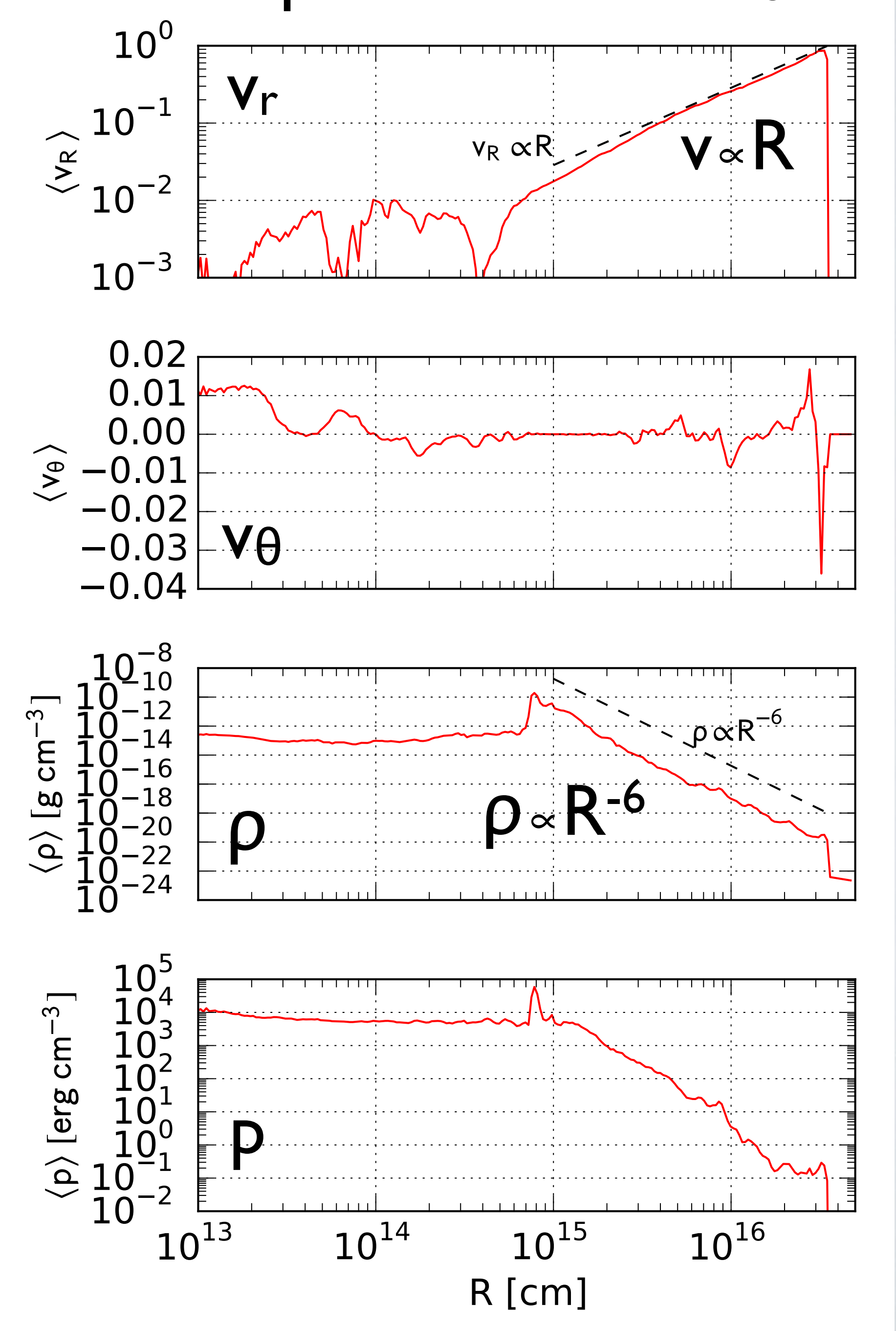

Early-time spectra

- blue continuum
- broad-line
- “w”-shape spectral feature (by [OII])

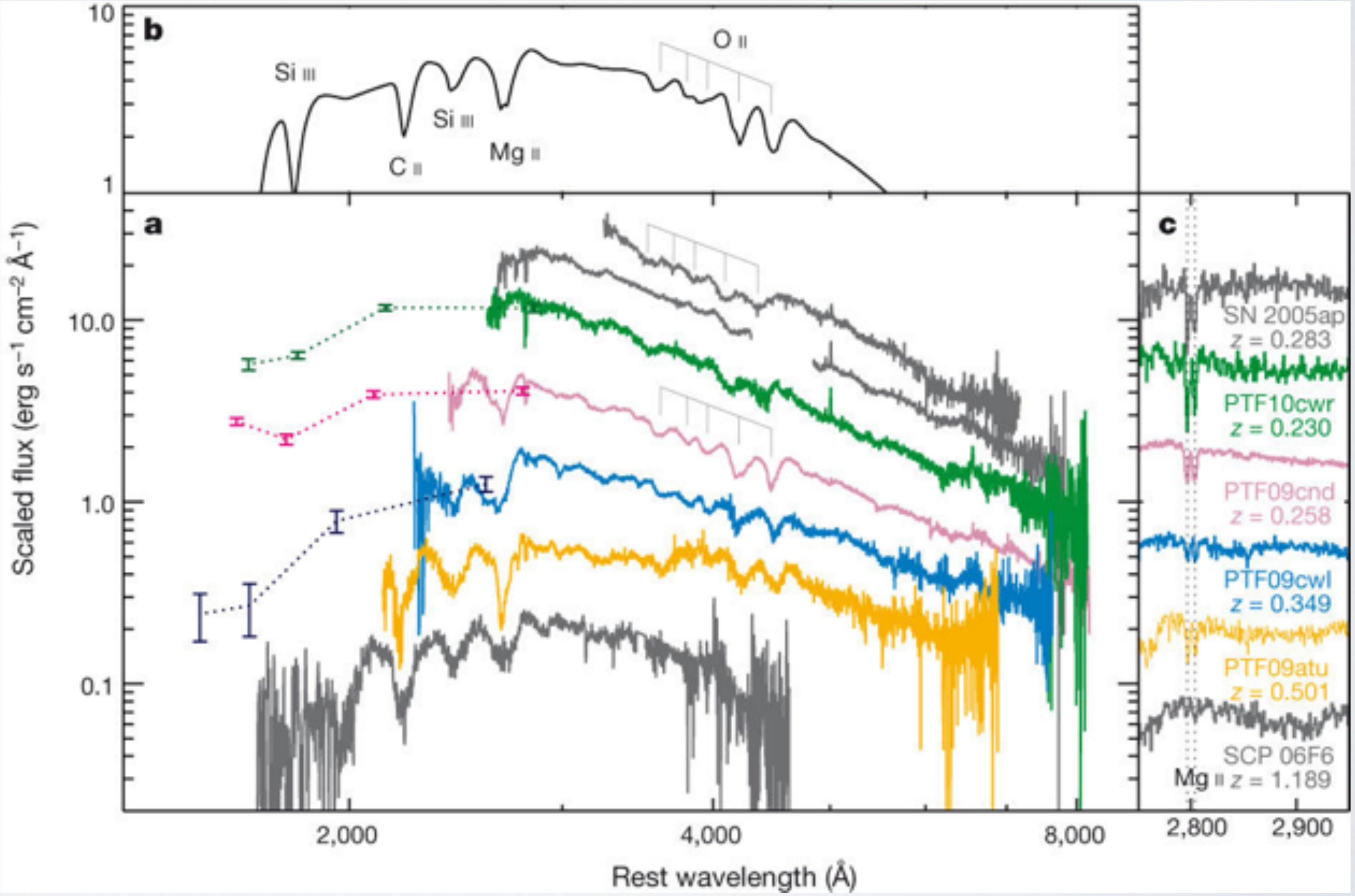

↑ SLSNe-I spectra (Quimby+ 2011)

Photospheric velocity evolution

- absorption features in SLSNe spectra is “broad”
- implied photospheric velocities are similar to Ic-BL SNe

  → large kinetic energy

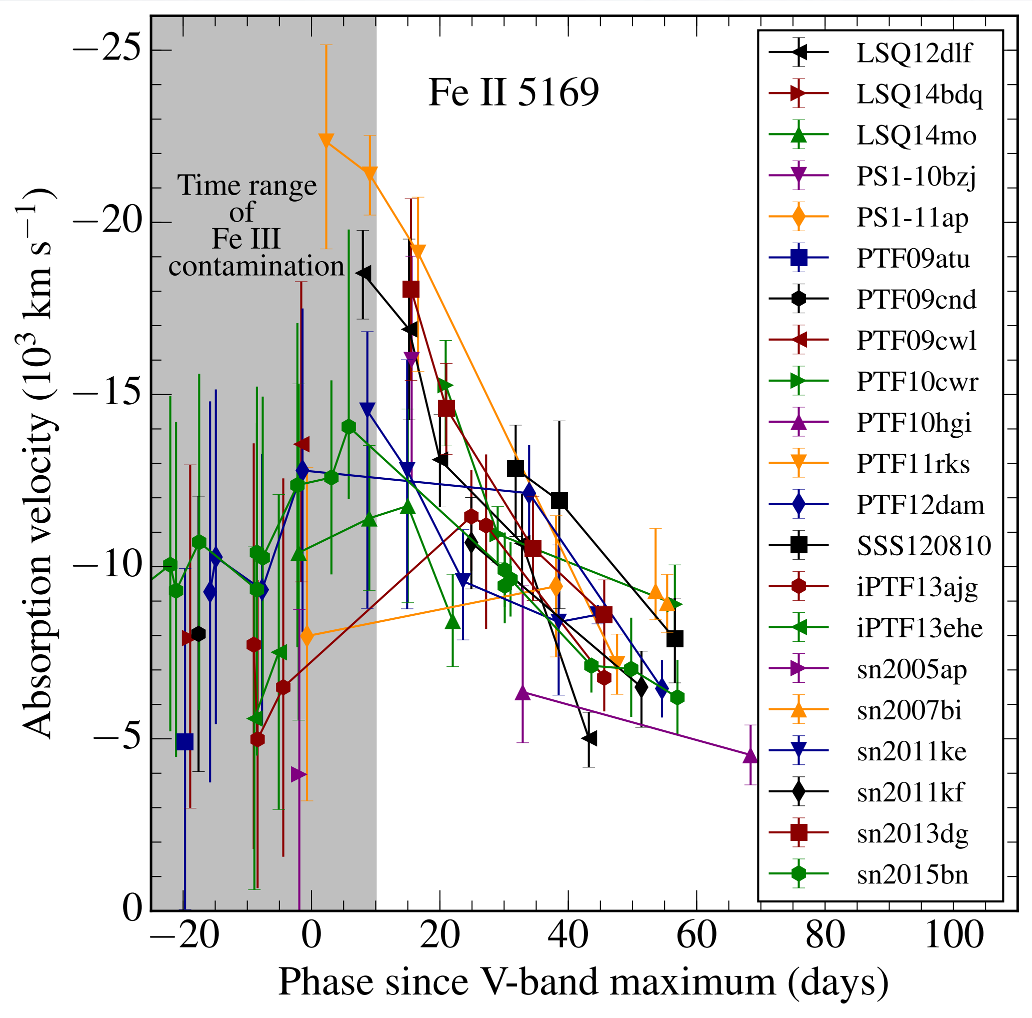

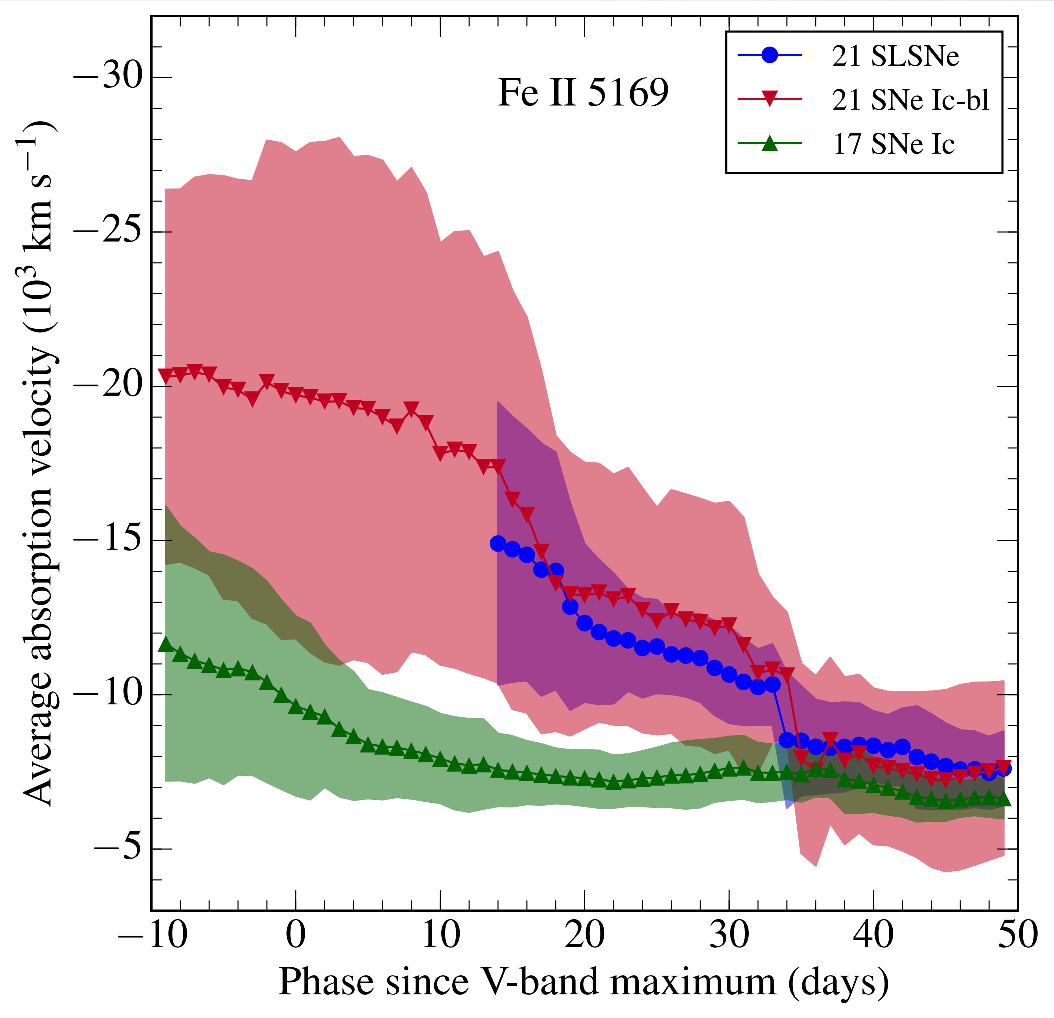

↑ averaged v_{ph} of SLSNe, Ic-bl Ic, and Ic SNe (Liu&Modjaz 2017)

Late-time spectra

- Late-time spectra of SNe are dominated by nebular lines
- ionization of elements by radioactive decay
- Nebular spectrum of SLSNe-I 2015bn similar to broad-lined Ic SNe? → severe line-blending
- a possible link between Ic-BL SNe and SLSNe-I?

Nicholl+ (2016)

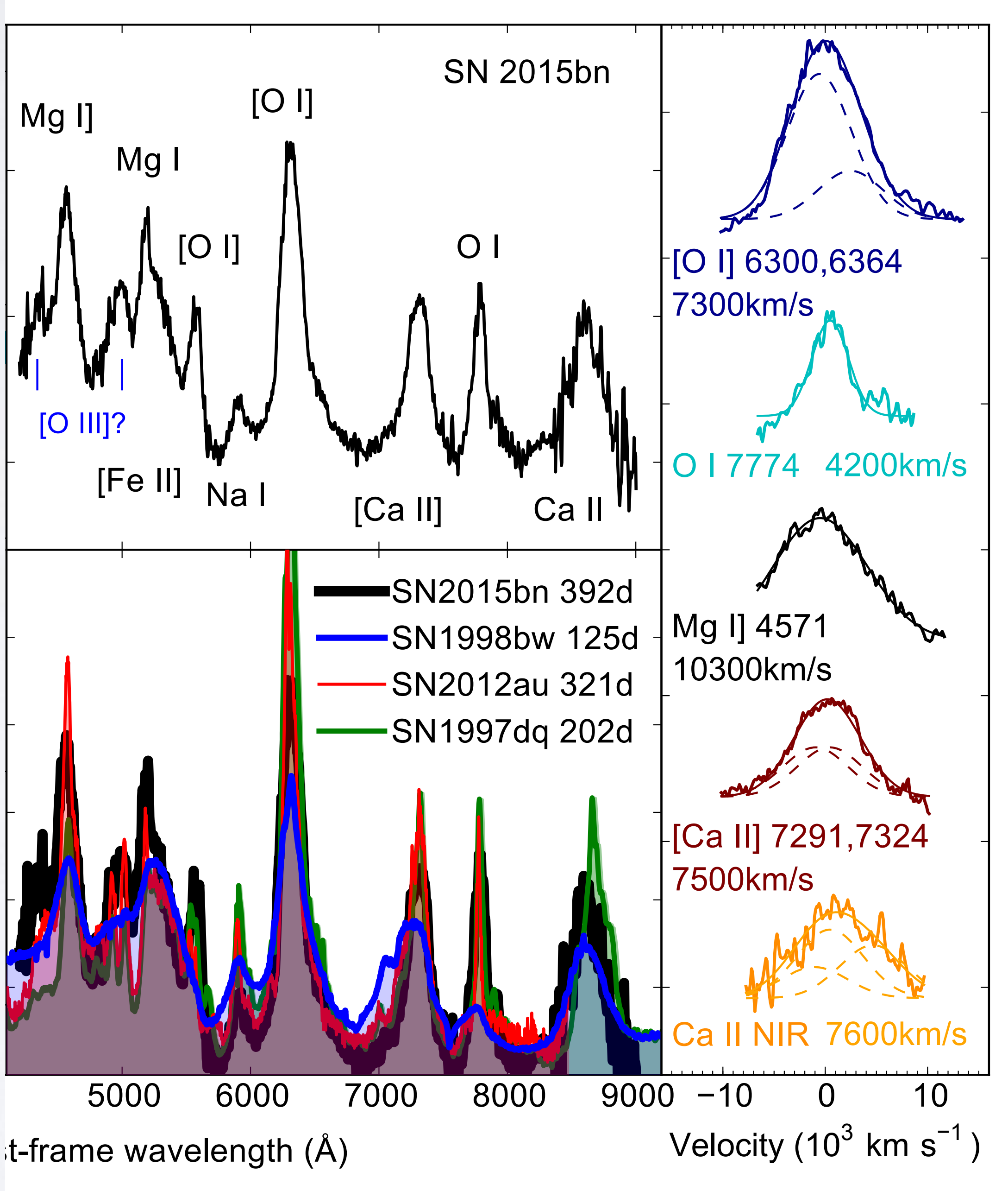

Event rate

- Lick Observatory Supernova Search (Li+2011)
  - CCSN rate @z=0 : ~10^{-4} SN Mpc^{-3} yr^{-1} = 10^5 SN Gpc^{-3} yr^{-1}
  - Ic-BL rate :~ 10^{-6} SN Mpc^{-3} yr^{-1} = 10^3 SN Gpc^{-3} yr^{-1}

- SLSNe volumetric rate @ z~0.1 (Quimby+2013)
  - SLSNe-I: 32^{+77}_{-26} SN $Gpc^{-3}yr^{-1}$
  - SLSNe-II: 151^{+151}_{-82} SN $Gpc^{-3}yr^{-1}$

- SLSNe-I volumetric rate @ z~1.0 = 91^{+76}_{-34} SN $Gpc^{-3}yr^{-1}$

- Ic-BL SNe are rare (~1% of CCSNe)
- SLSNe-I are extremely rare (~0.01-0.1% of CCSNe)

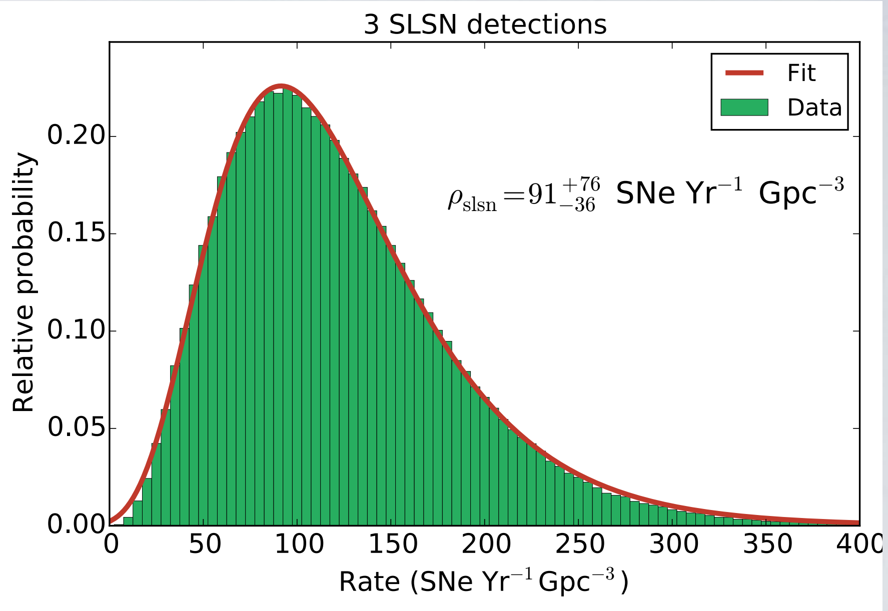

Figure 7. The probability distribution of the volumetric rate of SLSNe for the three SLSN candidates over the duration of SNLS at $0.2 < z < 1.6$, as determined by our 100,000 Monte Carlo simulations. A log-normal distribution is fitted to the data (red line) to estimate the peak of the probability distribution and the uncertainties, quoted as the 68% confidence region.

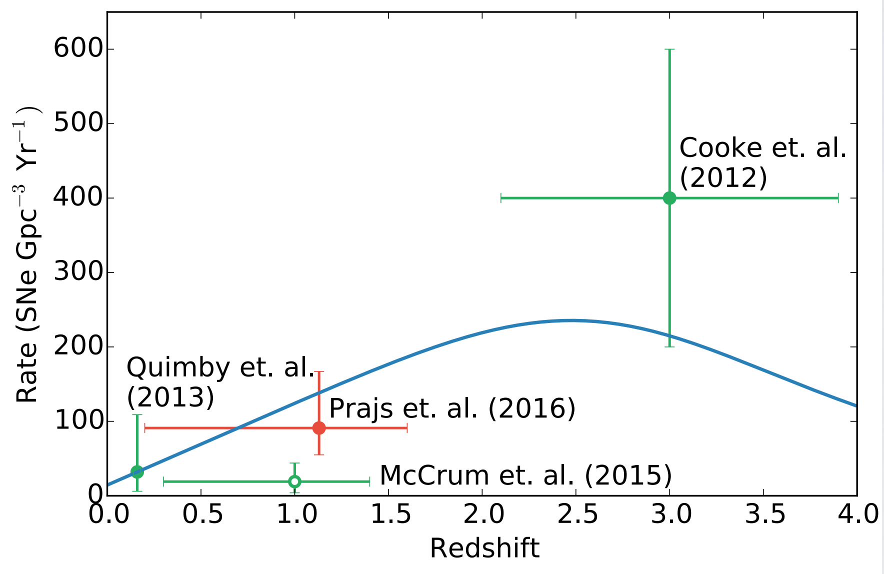

Figure 8. The evolution of the volumetric SLSN rate as a function of redshift. We show measurements by Quimby et al. (2013), McCrum et al. (2015) and Cooke et al. (2012) for comparison. The McCrum et al. (2015) result is marked by an open circle to highlight that it may not be directly comparable with the other measurements as it is derived by a comparison to the rate of core collapse supernovae and is not a direct measurement. The observed evolution is consistent with that of the SFH over the same redshift range; we over-plot in blue the parametrisation of the cosmic SFH of Hopkins & Beacom (2006), normalised to the low-redshift SLSN-I rate obtained by Quimby et al. (2013).

Host galaxy demographics

- star-forming dwarf galaxy (small stellar mass)
- high specific star formation rates (SFR/M★)
- low metallicity
- host galaxies of Ic-BL SNe and SLSNe-I are similar

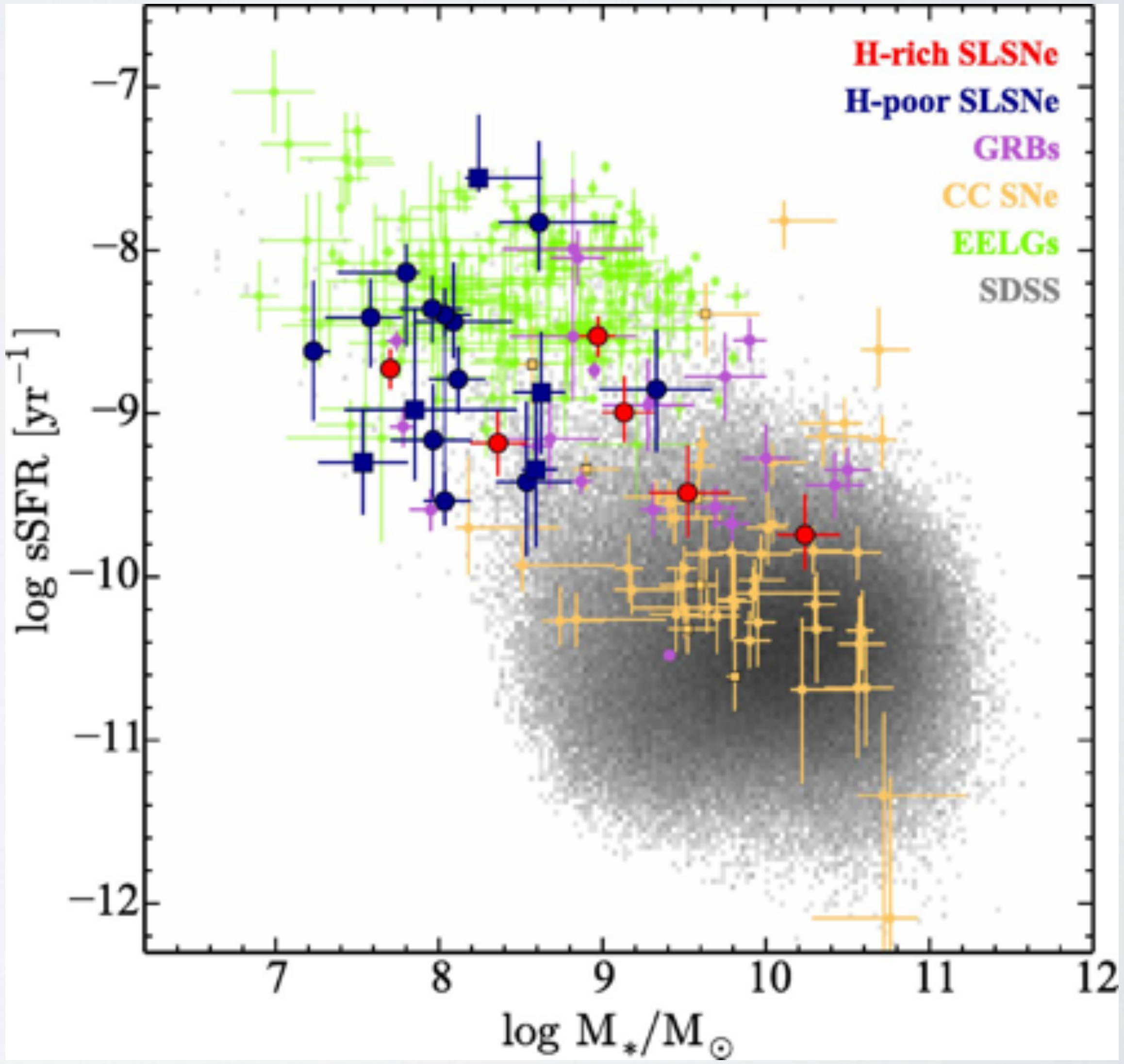

↑ stellar mass M★ vs sSFR (Leloudas+ 2015)

Host galaxy demographics

- star-forming dwarf galaxy (small stellar mass)
- high specific star formation rates (SFR/M★)
- low metallicity
- host galaxies of Ic-BL SNe and SLSNe-I are similar

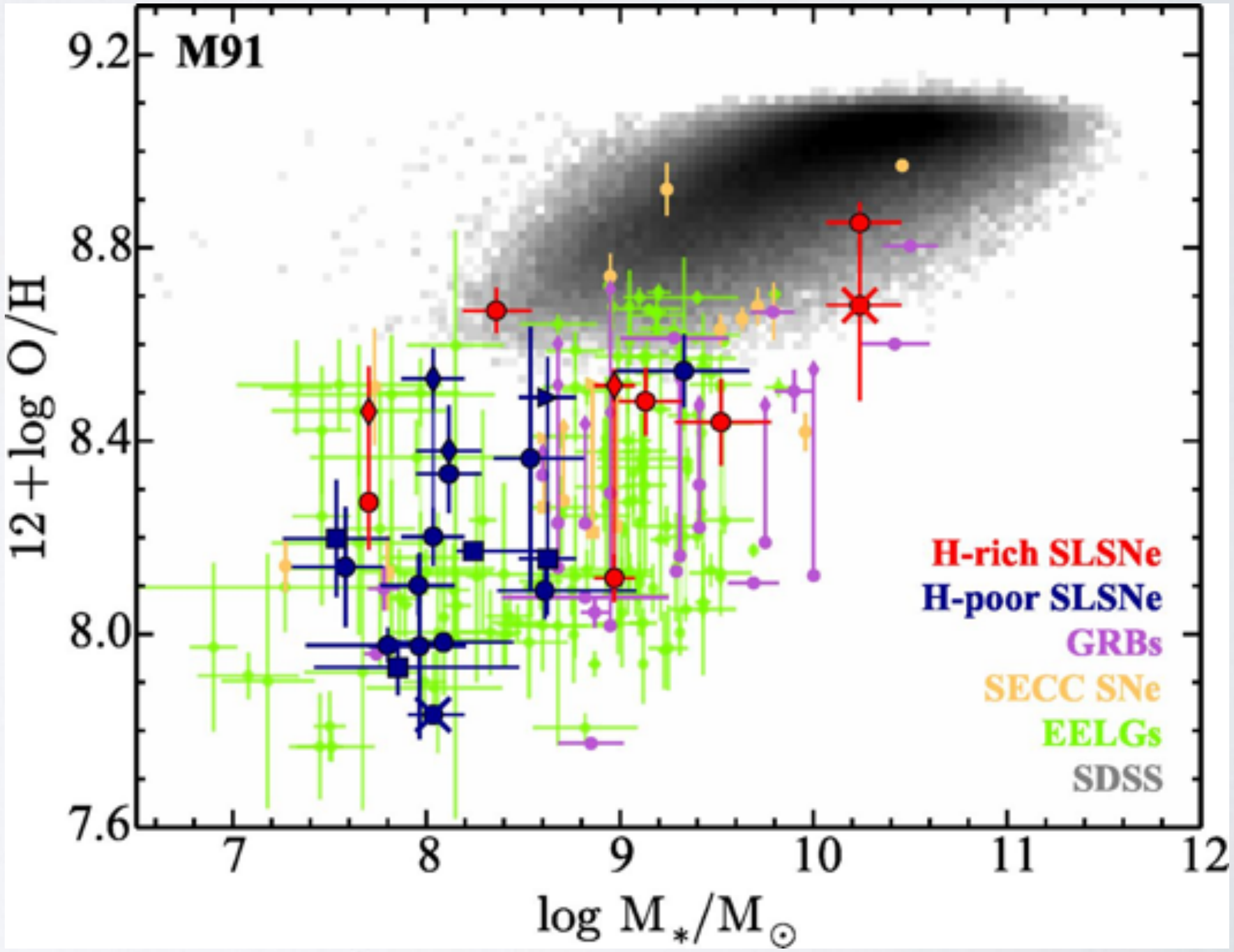

↑ stellar mass M★ vs metallicity (Leloudas+ 2015)